Award Number: DAMD17-01-1-0326

TITLE: Automated Method for Analysis of Mammographic Breast Density - A Technique for Breast Cancer Risk Estimation

PRINCIPAL INVESTIGATOR: Heang Ping Chan, Ph.D.

CONTRACTING ORGANIZATION: University of Michigan
Ann Arbor, Michigan 48109-5012

REPORT DATE: July 2003

TYPE OF REPORT: Annual

PREPARED FOR: U.S. Army Medical Research and Materiel Command
Fort Detrick, Maryland 21702-5012

DISTRIBUTION STATEMENT: Approved for Public Release;
Distribution Unlimited

The views, opinions and/or findings contained in this report are those of the author(s) and should not be construed as an official Department of the Army position, policy or decision unless so designated by other documentation.

20031114 080

REPORT DOCUMENTATION PAGE

Public reporting burden for this collection of information is estimated to average 1 hour per response, including the time for reviewing instructions, searching existing data sources, gathering and maintaining the data needed, and completing and reviewing this collection of information. Send comments regarding this burden estimate or any other aspect of this collection of information, including suggestions for reducing this burden to Washington Headquarters Services, Directorate for Information Operations and Reports, 1215 Jefferson Davis Highway, Suite 1204, Arlington, VA 22202-4302, and to the Office of Management and Budget, Paperwork Reduction Project (0704-0188), Washington, DC 20503

1. AGENCY USE ONLY (Leave blank)	2. REPORT DATE July 2003	3. REPORT TYPE AND DATES COVERED Annual (1 Jul 02 - 30 Jun 03)

4. TITLE AND SUBTITLE	5. FUNDING NUMBERS
Automated Method for Analysis of Mammographic Breast Density - A Technique for Breast Cancer Risk	DAMD17-01-1-0326

6. AUTHOR(S)
Heang Ping Chang, Ph.D.

7. PERFORMING ORGANIZATION NAME(S) AND ADDRESS(ES) University of Michigan Ann Arbor, Michigan 48109-5012 E-Mail: chanhp@umich.edu	8. PERFORMING ORGANIZATION REPORT NUMBER

9. SPONSORING / MONITORING AGENCY NAME(S) AND ADDRESS(ES) U.S. Army Medical Research and Materiel Command Fort Detrick, Maryland 21702-5012	10. SPONSORING / MONITORING AGENCY REPORT NUMBER

11. SUPPLEMENTARY NOTES

12a. DISTRIBUTION / AVAILABILITY STATEMENT Approved for Public Release; Distribution Unlimited	12b. DISTRIBUTION CODE

13. ABSTRACT (Maximum 200 Words)

The goal of this proposed project is to develop an automated technique to assist radiologists in estimating mammographic breast density.

During this project year, we have completed the analysis of the correlation between the percent mammographic dense area and the percent volumetric fibroglandular tissue measured on MR images. The performance of the automated segmentation program on the set of mammograms used in this study was verified with an experienced radiologist's manual segmentation. The percent mammographic dense area and percent volumetric fibroglandular tissue is highly correlated with correlation coefficients of 0.91 and 0.89, respectively, for CC and MLO views. The high correlation indicates the validity of using mammographic density as a surrogate for monitoring breast density changes. The computerized image analysis tool can provide a consistent and reproducible estimation of percent dense area on routine clinical mammograms, thereby contributing to the understanding of the relationship of mammographic density to breast cancer risk, detection, and prognosis, and the prevention and treatment of breast cancer.

We have also begun the development of an automated density segmentation method for direct digital mammograms (DMs). We performed a study to compare breast density estimated from digitized screen-film mammograms (SFMs) with that estimated from DMs. Our results indicate that breast density on DMs generally appears to be lower than that on SFMs because of the harder beam quality used and image processing applied to the DMs. The lower density may improve the mammographic sensitivity for lesion detection in dense breasts. However, for patients with SFMs and DMs taken over time, comparison of serial mammograms for breast density changes will be problematic. We are designing automated segmentation techniques for DMs. We will modify the program and evaluate its performance on DMs in the coming year.

14. SUBJECT TERMS Breast Cancer Mammography, breast density, computer-assisted analysis, automated segmentation, risk monitoring	15. NUMBER OF PAGES 54
	16. PRICE CODE

17. SECURITY CLASSIFICATION OF REPORT Unclassified	18. SECURITY CLASSIFICATION OF THIS PAGE Unclassified	19. SECURITY CLASSIFICATION OF ABSTRACT Unclassified	20. LIMITATION OF ABSTRACT Unlimited

Table of Contents

(4) Introduction

Previous studies have found that there is a strong correlation between mammographic breast density and the risk of breast cancer. Mammographic breast density has been used by researchers in many studies to estimate breast cancer risk of epidemiological factors, monitor the effects of preventive treatments such as tamoxifen or dietary interventions, monitor the breast cancer risk of hormone replacement therapy, and investigate factors affecting mammographic sensitivity and cancer prognosis. However, most studies used Breast Imaging Reporting and Data System (BI-RADS) density rating as a measure of mammographic breast density, which contributes large inter- and intraobserver variations and may reduce the sensitivity of the analysis.

The goal of this proposed project is to develop a fully automated technique to assist radiologists in estimating mammographic breast density. We hypothesize that the computerized technique can accurately and efficiently segment the dense area on digitized or digital mammograms, thereby eliminating inter- and intra-observer variations. The dense area as a percentage of total breast area thus estimated will be more consistent and reproducible than radiologists' subjective BI-RADS rating. To accomplish this goal, we will (1) collect a large database of mammograms, including digitized film mammograms and digital mammograms, for training and testing the dense area segmentation program; (2) evaluate the correlation between the radiologists' breast density classification based on BI-RADS lexicon and the percent breast dense area; and (3) study the correlation of percent breast dense area between different views of the same breast and between the same view of the two breasts; and (4) investigate the correlation between the percent breast dense area estimated from mammograms and the volumetric dense breast tissue estimated from a data set of magnetic resonance (MR) breast images. These comparisons will provide important information regarding the consistency of the BI-RADS rating with the measured percent breast dense area, the appropriate measure of % dense area from different mammographic views, and the usefulness of using the percent breast dense area on mammograms as an indicator of volumetric breast tissue density.

It is expected that this project will produce a fully automated and effective tool for analysis of mammographic breast density, which can be applied to routinely acquired mammograms without special calibrations. This will facilitate studies of various factors associated with breast cancer risk and mammographic sensitivity, and monitoring the effects of interventional or preventive strategies. The image analysis tool will therefore contribute to the understanding of the relationship of density to breast cancer risk, detection, prognosis, and to the prevention and treatment of breast cancer.

(5)   Body

In the current project year (7/1/02-6/30/03), we have performed the following studies:

(A)   Investigation of Correlation between Volumetric Fibroglandular Tissue on MR Images and Mammographic Density

(a)   Collection of a Database MR Breast Images with Corresponding Mammograms

As discussed in the progress report last year, with IRB approval, we collected a data set of breast images from the research files of a previous project that included magnetic resonance (MR) images and corresponding mammograms. In the MR study, patients were scanned prone using a commercial dual phased-array breast coil. The imaging protocol included a coronal three-dimensional (3D) T1-weighted pre-contrast series (coronal sections 2-5 mm thick, 32 slices; 3D Spoiled Gradient-Recalled Echo (SPGR); TE=3.3 ms; TR=10 ms, Flip=40°, matrix=256×128, FOV=28-32 cm right/left, 14-16 cm superior/inferior, scan time=2 min 38 sec). This 3D SPGR sequence produces full volume coverage of both breasts with contiguous image sections. The dense parenchyma and fat tissue are well separated with this heavily T1-weighted acquisition. We used a set of 67 patients to study the correlation between the 2-D projected percentage of dense area on a mammogram and the percentage of dense tissue volume estimated from the 3-D MR images.

The mammograms consisting of the craniocaudal (CC) view and the mediolateral oblique (MLO) view of both breasts of the patient were digitized with a LUMISYS 85 laser film scanner at a pixel size of $50 \mu m \times 50 \mu m$. The digitizer has a gray level resolution of 12 bits and a nominal optical density range of 0 to 4. For density segmentation, it is not necessary to use high resolution images. To reduce processing time, the full resolution mammograms were smoothed with a 16×16 box filter and subsampled by a factor of 16, resulting in $800 \mu m \times 800 \mu m$ images for this study.

In the previous progress report, we described the graphical user interface (GUI) developed in this project for semi-automatic segmentation of the fibroglandular tissue in the MR images. We also discussed the preliminary results after analysis of the images of 37 patients. In the current project year, we continued the analysis and completed the study of 67 patients. An observer experiment in which two experienced radiologists manually segmented the mammographic density by interactive thresholding was also performed and compared with the computerized segmentation. The study was submitted as a journal article to the *Medical Physics* Journal (ref. 1). These analyses are summarized in this report.

(b)   Estimation of Fibroglandular Tissue Volume on MR Images

Our algorithm for segmentation of volumetric fibroglandular tissue on MR images employs a semi-automatic method. This method, implemented in a GUI, was discussed in detail in the progress report last year. The method is briefly summarized below.

The computer first performs an initial segmentation. The GUI allows a user to review the segmentation of every slice by the computer and make modifications if necessary. The method

consists of four steps. First, the breast boundary is detected automatically on each slice. A deformable model and manual modification are used to correct for incorrectly detected boundaries that usually occur in slices near the chest wall where there are no well-defined breast boundaries. Because of inhomogeneity of the breast coil sensitivity, the signal intensity in the breast region is not uniform across the field of view. A background correction technique that estimates the low frequency background from the gray levels along the breast boundary is developed to reduce this systematic nonuniformity. Manual interactive thresholding of the gray level histogram in the breast region is then used to separate the fibroglandular from the fatty region. Morphological erosion is used to exclude the skin voxels along the breast boundary. After the fibroglandular tissue is segmented for each slice, the total number of voxels containing the fibroglandular tissue is obtained as a summation of these voxels over all slices of the breast. The total volume of the breast is obtained as the summation of the voxels enclosed by the breast boundary before morphological erosion. The ratio of these two volumes provided the percent volumetric fibroglandular tissue in the breast. A flow chart of our algorithm is shown in Fig. 1.
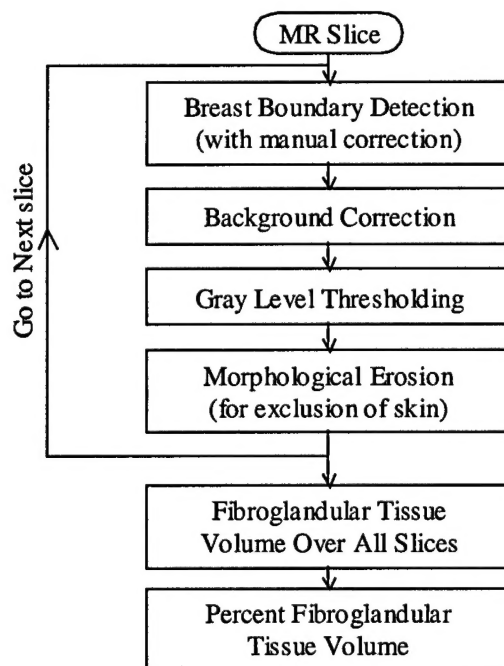

Fig. 1 The flow-chart for the segmentation of fibroglandular tissue on MR images.

(c)   Mammographic Density Segmentation

We have previously developed an automated method for segmentation of the dense fibroglandular area on mammograms. The method, referred to as the Mammographic Density ESTimator (MDEST), was described in detail in the journal article enclosed in last year's report (ref. 2). In brief, the breast boundary on the digitized mammogram is tracked. A dynamic-range compression technique reduces the gray level range of the breast area. By analyzing the shape of the gray level histogram, a rule-based classifier classifies the breast density into one of four classes. Typically, a Class I breast is almost entirely fat, it has a single narrow peak on the histogram. A Class II breast contains scattered fibroglandular densities. Its histogram has two

main peaks, with the smaller peak on the right of the bigger one. A Class III breast is heterogeneously dense. Its histogram also has two peaks, but the smaller peak is on the left of the bigger one. A Class IV breast is extremely dense. Its histogram has mainly a single dominant peak, but the peak is wider compared with the peak in the Class I histogram. A second smaller peak sometimes occurs on the left of the main peak. Based on the histogram shape, a threshold is automatically calculated to separate the dense and fatty pixels. The mammographic density was estimated as the percentage of fibroglandular tissue area relative to the total breast area. For MLO view mammograms, the pectoral muscle is detected and excluded from the density area or breast area calculations. In our previous work (ref. 2), the performance of MDEST was verified by comparison with manual segmentation by 5 breast imaging radiologists using a data set of 260 mammograms from 65 patients that were different from the cases used in the current study. We found that the correlation between the computer-estimated percent dense area and the average segmentation by the 5 radiologists was 0.94 and 0.91, respectively, for CC and MLO views, with a mean bias of less than 2%.

MDEST was applied to the mammograms of the 67 patients used in this study. The percent dense area on mammograms was estimated for the CC-view and the MLO-view mammogram of each breast separately. In addition, an MQSA approved radiologist also segmented the dense area by interactive thresholding for each mammogram. The correlation between the mammographic density obtained by manual and automatic segmentation is shown in Fig. 2(a) and 2(b) for the CC view and MLO view, respectively. The correlation coefficients were 0.91 and 0.91, respectively, for the CC view and MLO view. The mammographic densities estimated by automatic and manual segmentation were compared with the percent volumetric fibroglandular tissue on MR images as described below.
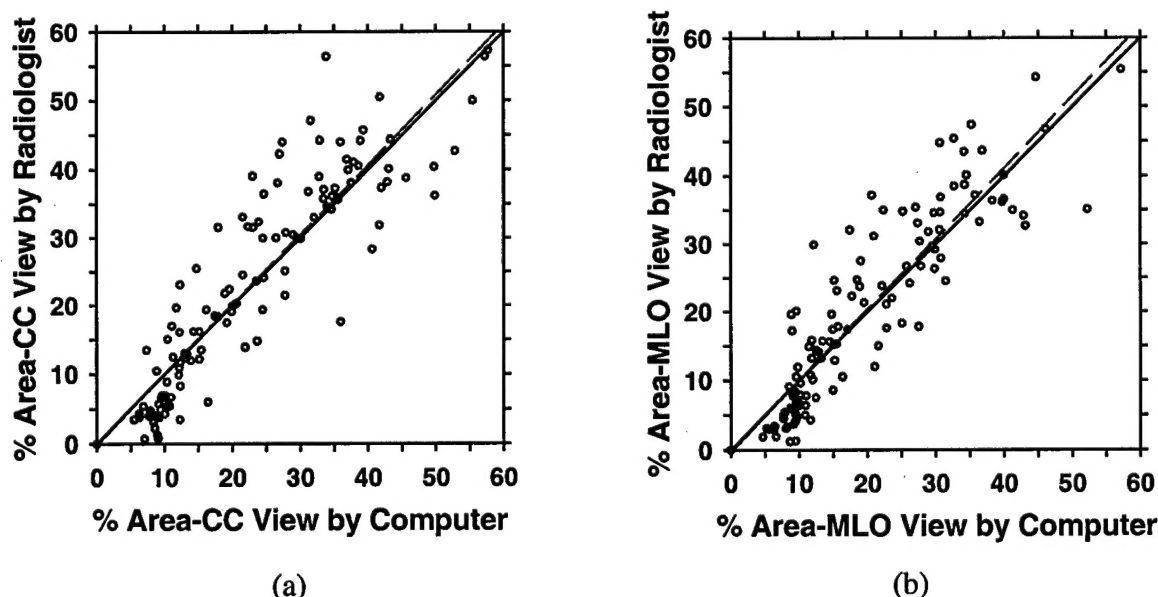

(a)   (b)

Fig. 2   Comparison of the percent mammographic density obtained from interactive thresholding by an MQSA radiologist and that estimated by our automated MDEST computer program. (a) CC view, correlation coefficient = 0.91 (b) MLO view, correlation coefficient = 0.91. Dash line: linear regression of the data; solid line: diagonal.

(d)   Observer Experiments for Segmentation of MR Breast Images

We performed observer experiments to evaluate the inter-observer variations in the segmentation of fibroglandular tissue using the semi-automatic method. Twenty-three MR cases from the data set were randomly selected for this observer experiment. There were a total of 41 breasts because some cases had only one breast. Two MQSA approved radiologists performed the segmentation of the fibroglandular tissue on MR images using the semi-automatic method implemented with the GUI. A non-radiologist researcher who was trained by these radiologists also performed the segmentation independently with the GUI.

After verifying the consistency of segmentation by these observers, the trained researcher completed the segmentation of all MR cases. The correlation between percent volumetric fibroglandular tissue on MR images and percent dense area on mammograms was then examined for the entire data set.

<u>Inter-observer variation between radiologists</u>

Fig. 3 shows the comparison of the percent volumetric fibroglandular tissues on MR images segmented by two radiologists for the 41 breasts. The correlation between the segmentation results of the two radiologists is 0.99. To compare the difference between their results, the mean difference and the root-mean-square (RMS) residual, which is the residual from the linear least-squares-fitted line, was also calculated. The mean difference was found to be 0.7 and the RMS residual was 1.4.
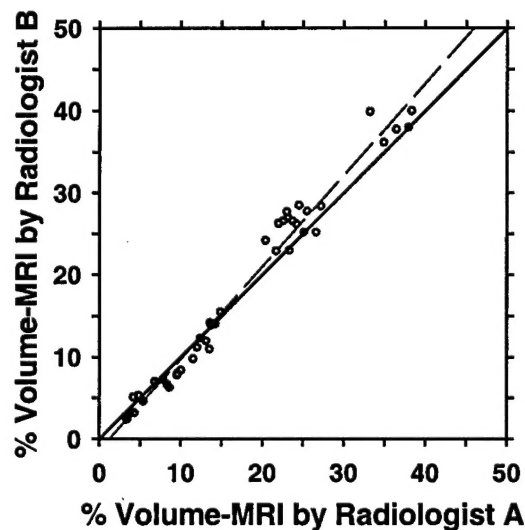

Fig. 3   Comparison of the segmentation of fibroglandular tissue from MR images between two experienced MQSA radiologists, correlation coefficient = 0.99. Dash line: linear regression of the data; solid line: diagonal.

Inter-observer variation between radiologists and trained non-radiologist researcher

Fig. 4 showed the comparison of the percent volumetric fibroglandular tissues segmented by the trained non-radiologist against those segmented by the two radiologists. The correlation between the result of the trained non-radiologist and the results of both radiologists was 0.99. The corresponding mean differences were 0.8 and 0.5, respectively, and the RMS residuals were 1.2 and 0.5, respectively.
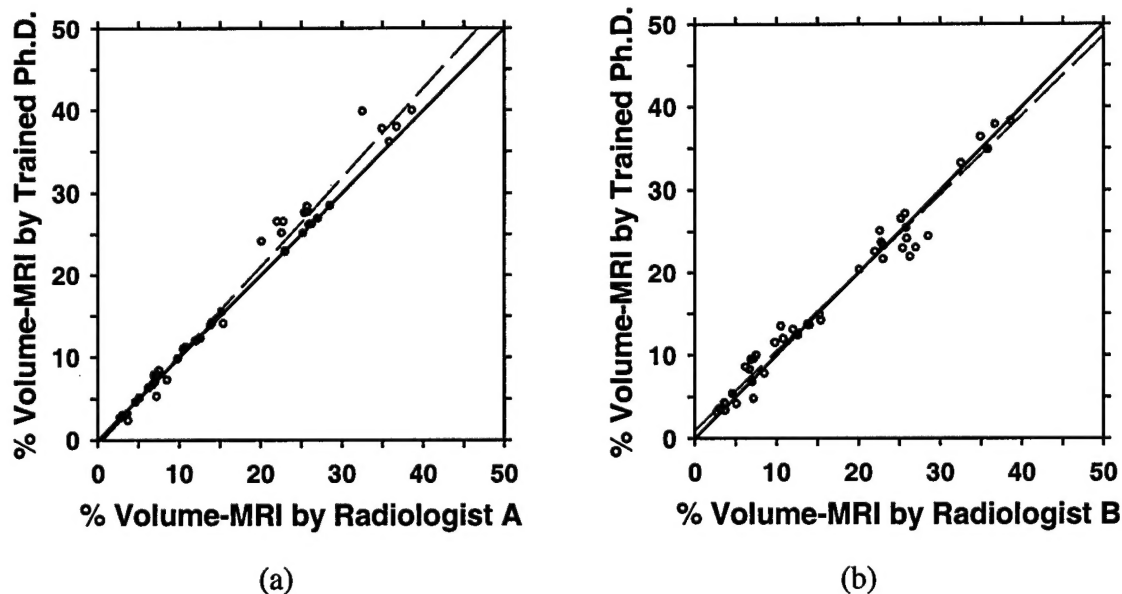

| (a) | (b) |

Fig. 4   Comparison of the segmentation of fibroglandular tissue from MR images between the trained non-radiologist and two experienced MQSA radiologists. (a) Radiologist A, correlation coefficient = 0.99, (b) Radiologist B, correlation coefficient = 0.99. Dash line: linear regression of the data; solid line: diagonal.

(e)   Analysis of Correlation between Volumetric Fibroglandular Tissue on MR Images and Mammographic Density

The percent volumetric fibroglandular tissue on MR images was compared with the percent dense area on CC- and MLO-view mammograms. After verifying that the difference in segmentation between the trained non-radiologist and the radiologists was similar to the interobserver variations between the two experienced radiologists, the trained non-radiologist completed the segmentation of the entire data set.

Fig. 5 shows the comparison of the percent volumetric fibroglandular tissue on MRI and the percent mammographic density segmented by a radiologist. The percent areas on CC- and MLO-view mammograms are higher than the percent volume on MR images by 5.7% and 3.0%, respectively.

Fig. 6 shows the comparison of the percent volumetric fibroglandular tissue on MRI and the percent mammographic density segmented by MDEST. The percent areas on CC- and MLO-

view mammograms segmented by the computer are higher than the percent volume on MR images by 5.2% and 2.6%, respectively.
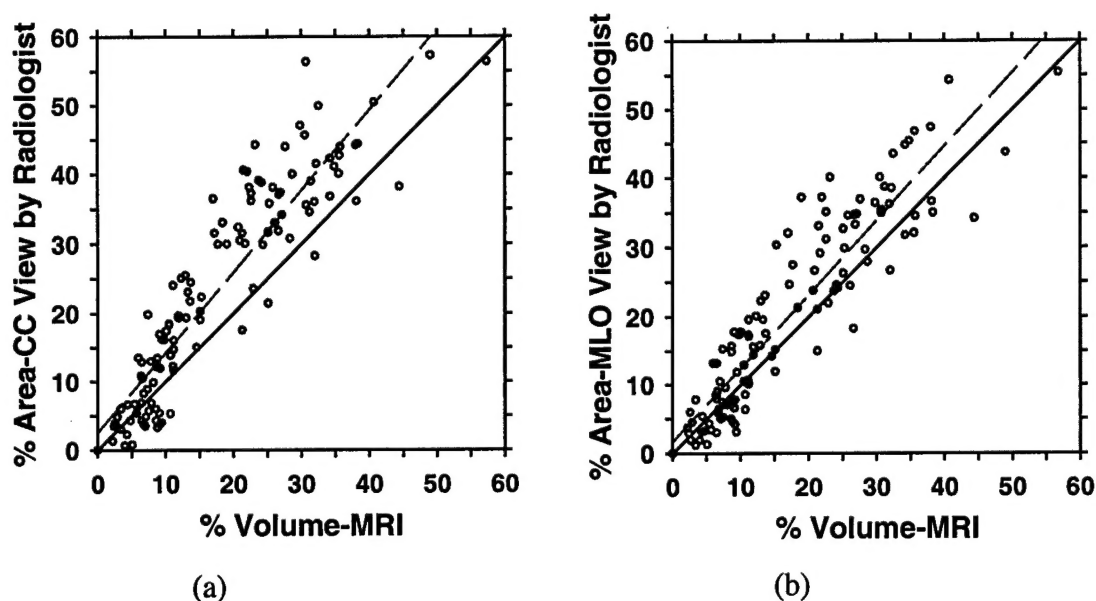

Fig. 5 Comparison of the percent fibroglandular tissue volume on MR images and the percent dense area on mammograms segmented by an experienced radiologist. (a) CC view, correlation coefficient = 0.91, (b) MLO view, correlation coefficient = 0.91. Dash line: linear regression of the data; solid line: diagonal.
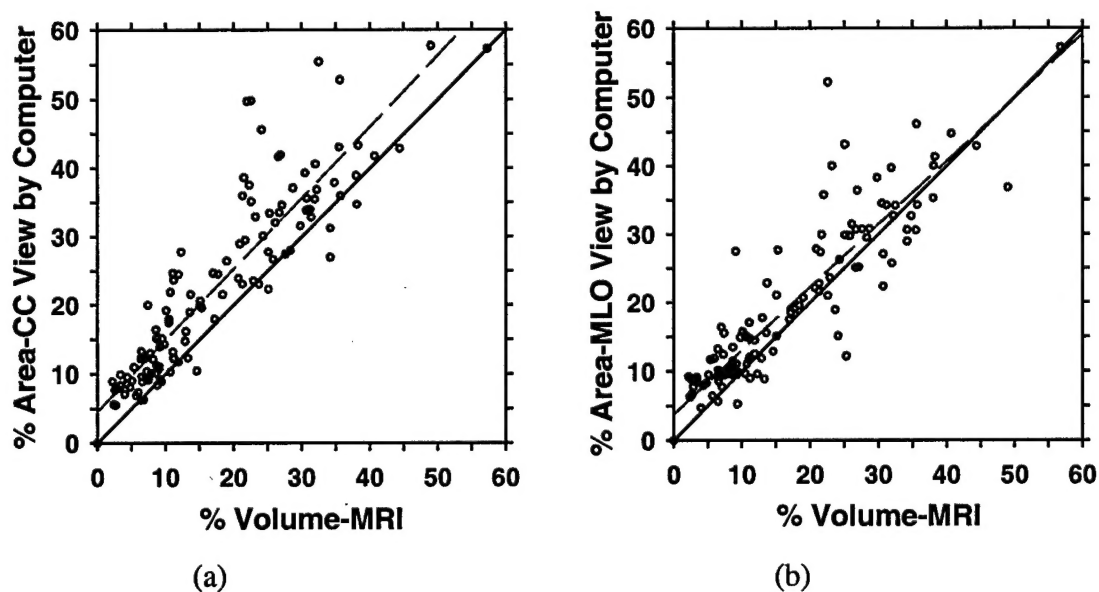

Fig. 6 Comparison of the percent volume on MR images and the percent area on mammogram segmented by our automated MDEST computer program. (a) CC view, correlation coefficient = 0.91, (b) MLO view, correlation coefficient = 0.89. Dash line: linear regression of the data; solid line: diagonal.

The correlation coefficients, the mean differences, and the RMS residuals between the percent volumetric fibroglandular tissue on MR images and percent dense area on mammograms are compared in Table. 1. The correlation between the percent volume on MR images and percent area on mammograms of the fibroglandular breast tissue is high, ranging from 0.89 to 0.91. Although it is not expected that the values of percent volume agree with the values of percent area, their mean differences range only from 3% to 6%.

Table 1. Statistic analysis of the relationship between percent fibroglandular tissue volume on breast MR images and percent dense area on mammograms segmented by radiologist and MDEST.

	Radiologist		Computer (MDEST)	
	CC vs MRI	MLO vs MRI	CC vs MRI	MLO vs MRI
Correl. Coeff.	0.91	0.91	0.91	0.89
RMS Residual	6.3	5.6	5.8	5.4
Mean Diff.	5.7	3.0	5.2	2.6

The density on mammograms is a 2D projected area of the fibroglandular tissues. The percent dense area is not expected to be equal in value to the percent volume. The average differences between the percent volume and the percent area on CC and MLO views, as determined by the radiologist's interactive segmentation, are 5.7 and 3.0, respectively (Table I), with the percent dense area values being higher. We also investigated the RMS residual between the percent volume and the percent area when the relationship between them was assumed to be linear. The RMS residual between the percent volume and the percent area on CC and MLO views are 6.3 and 5.6, respectively (Table I), relative to the straight line obtained from linear least squares fits to the data. One possible factor that may contribute to a higher value of percent dense area on mammograms than the percent volume value on MR images is that the tissue volume imaged by the two modalities is somewhat different. The MR images include more tissue near the chest wall, which is mainly retroglandular adipose tissue, than a mammogram does, thus reducing the percent fibroglandular tissue volume.

Geometrically, we do not expect the relationship between volume and its projected 2D area to be linear. In a hypothetical situation such that the dense tissue volume is a sphere (volume $= \frac{4}{3}\pi r^3$) enclosed inside a concentric spherical shell of fatty tissue volume, the percent projected 2D area (area $= \pi r^2$) of the inner sphere relative to the outer sphere is equal to the percent volume to the power of 2/3. The relationship between the percent area and the percent volume is therefore not linear, and the percent area is larger in value than the percent volume for any ratio of radii between the two spheres. In general, the compressed breast and the dense tissue are not spherical. To investigate the empirical relationship between the percent area and the

percent volume in the nonlinear situation, we applied least squares fits in several polynomial models to the data points in Fig. 5. The results are shown in Table 2 and Fig. 7. Comparison of Table 1 and Table 2 indicates that the $Y = kx^{2/3}$ model, (x=percent fibroglandular tissue volume, Y=percent mammographic dense area) resulted in slightly larger RMS residuals than the linear model. The model $Y = kx^m$ with m equal to 0.83 and 0.86, respectively, for CC and MLO views slightly reduced the RMS residuals. The best fit was obtained from the model $Y = k_1x^m + k_2$. However, the situation that the percent projected area was negative when the percent volume was zero would not occur physically. Note that if the model was fitted to the percent area data segmented by MDEST (Fig. 6), the k_2 values would become positive, indicating that the non-zero k_2 values are likely caused by segmentation biases.

Overall, these models demonstrate that there is no simple mathematical relationship between the percent volume and the percent projected area but the values for the exponents appeared to be in a reasonable range. The relationship between the percent volume of two 3D objects, one within another, and their percent projected 2D area depends on their shapes. For example, the closer the two volumes are to concentric cylinders of the same height, the closer the exponent is to unity. The spread of the data points can therefore be attributed to the various irregular shapes of the fibroglandular tissue in the breasts, the changes in the shapes of the fatty and fibroglandular tissue due to compression, as well as the uncertainties in segmentation of both the mammograms and the MR images. Nevertheless, the strong correlation observed between the percent dense area on mammograms and the percent volumetric fibroglandular tissue on MR images indicates that mammographic density can be used as a surrogate for percent fibroglandular tissue volume for monitoring changes in breast density.
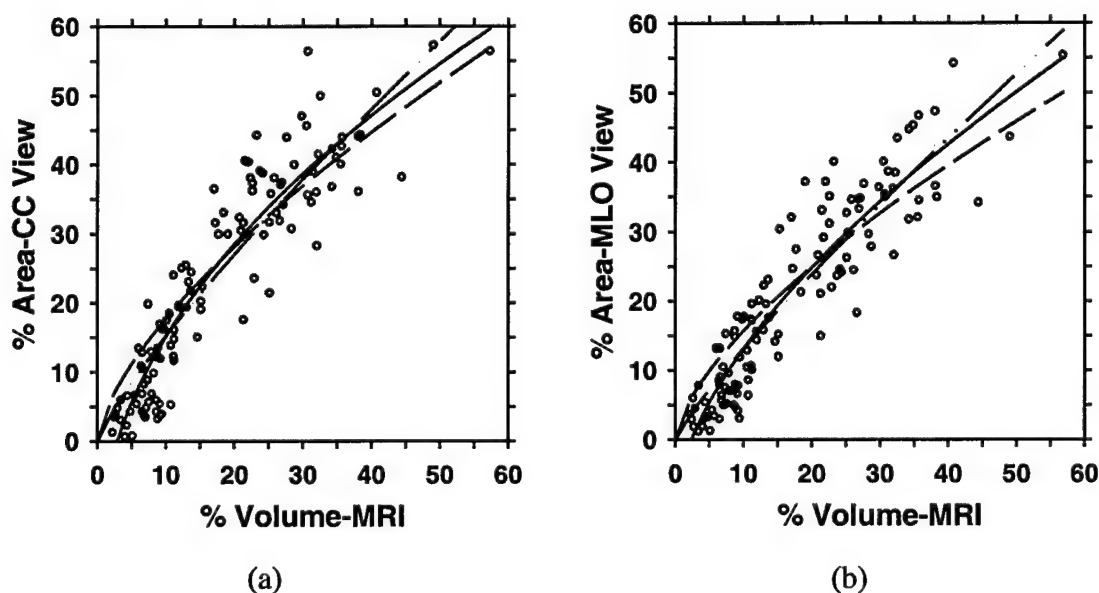

Fig. 7 Nonlinear fitting of the relationship between the percent volume and the percent area segmented by radiologist with least squares method. (a) CC view, (b) MLO view. Dash line: $y = kx^{2/3}$; dash-dot-dot line: $y = kx^m$; solid line: $y = k_1x^m + k_2$. The fitted parameters of the models, m, k, k_1 and k_2, are shown in Table 2.

Table 2. Analysis of the relationship between percent fibroglandular tissue volume (x) on breast MR images and percent dense area (Y) on mammograms segmented by radiologist using three mathematical models. m, k, k_1 and k_2 are constants determined by least squares curve fitting.

Mathematical Model		$Y = kx^{2/3}$	$Y = kx^m$	$Y = k_1 x^m + k_2$
CC vs MRI	Least Squares Fit	$Y = 0.82x^{2/3}$	$Y = 1.03x^{0.83}$	$Y = 1.02x^{0.48} - 0.19$
	RMS Residual	6.5	6.0	5.6
	Coefficient of determination	0.82	0.85	0.87
MLO vs MRI	Least Squares Fit	$Y = 0.73x^{2/3}$	$Y = 0.96x^{0.86}$	$Y = 0.90x^{0.60} - 0.09$
	RMS Residual	6.0	5.5	5.3
	Coefficient of determination	0.80	0.84	0.85

(B)   Comparison of Breast Density Estimated on Digitized Screen-Film Mammograms and Full Field Digital Mammograms

Digital mammographic systems have recently been introduced into clinical use. We performed a preliminary study to compare the breast density estimated on pairs of digital mammogram (DM) and digitized screen-film mammogram (SFM) obtained from the same patients. This study will provide information on the design of an automated breast density segmentation method for digital mammograms.

(a)   Collection of a Database of Full Field Digital Mammograms

We are comparing image information on DMs and SFMs for radiologist's interpretation and computerized image analysis. One hundred forty-five pairs of DM and SFM (76 CC views and 69 MLO views) were collected with IRB approval from 68 patients. The time interval between the DM and SFM ranged from 0 to 118 days (median=21 days). The SFMs were acquired with GE DMR systems and the DMs were acquired with the GE Senographe 2000D system. Both the DMs and the SFMs were acquired with automated exposure techniques that selected the appropriate target, filter, and kVp. The SFMs were digitized with a laser film

scanner. The breast boundaries on the DMs and SFMs were detected automatically by the computer. The mammograms were displayed on a workstation with a graphical user interface (see Fig. 6) that allowed interactive thresholding of the gray level histograms to segment the dense region from the fatty region. The DMs and SFMs were segmented independently in separate sessions so that the observer could not compare the density of the corresponding DM and SFM. Hard copies of the displayed images were available for reference during segmentation. The mammographic density was estimated as the percent dense area relative to the breast area, excluding the pectoral muscle in the MLO views.

(b)   Graphical User Interface for Segmentation of Breast Density on Digital Mammograms

We have previously developed a GUI for interactive thresholding of dense tissue regions on SFMs. The GUI is used in observer experiments so that radiologists can segment the mammograms manually and provide a gold standard for developing automated computerized segmentation methods. We have modified the GUI for SFMs to be used with DMs. In this preliminary study, we used the new GUI for DMs to manually segment a data set of DMs. The results are compared with manual segmentation of SFMs of the same patients, described above, using the previously developed GUI. An example of density segmentation for a DM with interactive thresholding using the GUI is shown in Fig. 8.
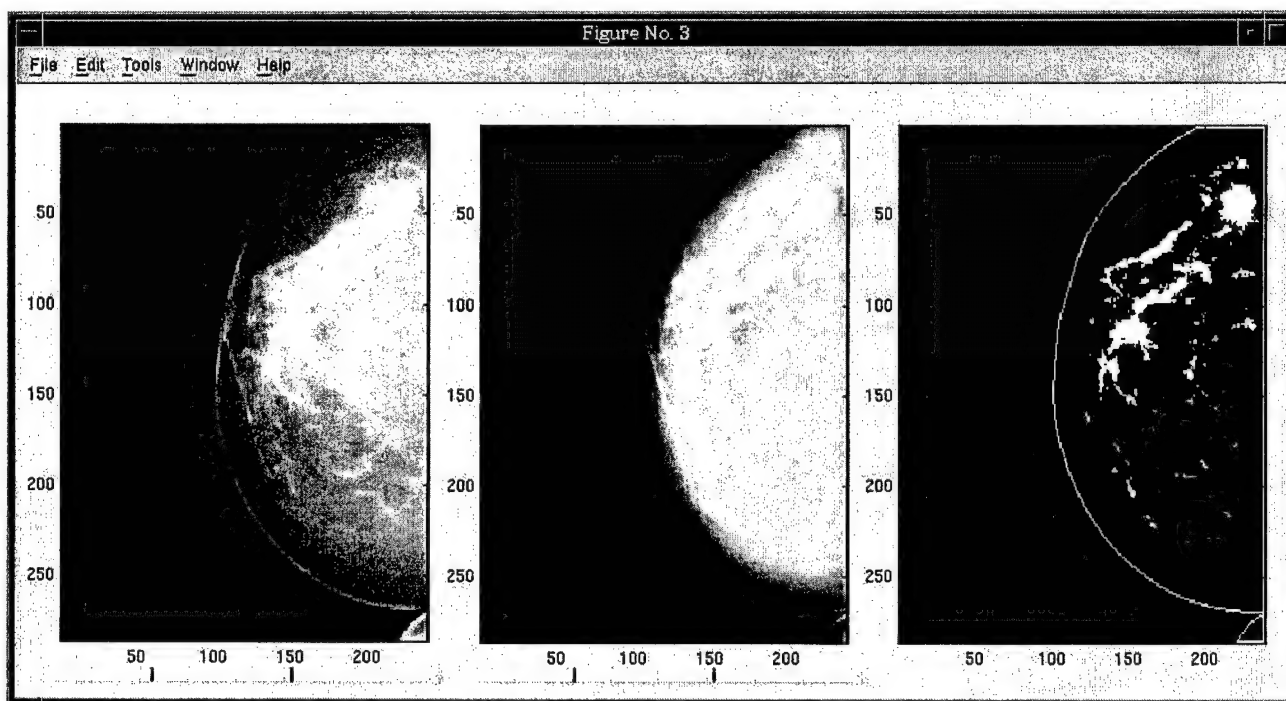

Fig. 8. An example of density segmentation on digital mammograms. Left: GE processed image. Middle: Our processed image. Right: segmentation result of breast density.

(c) **Correlation between Breast Density Estimated on Digitized Screen-Film Mammograms and Full Field Digital Mammograms**

Fig. 9 shows the comparison of the percentage area of breast density on both digitized SFMs and DMs by an observer. The correlation between the mammographic density on SFM and DM was 0.94 and 0.92, the root-mean-square residual was 4.5% and 4.6%, and the average ratio of mammographic density estimated on SFM to that on DM of the same breast was 1.18 and 1.22, respectively, for CC and MLO views. The differences in the percent dense area between the DM and SFM were statistically significant (paired t test: $p < 0.0000001$) for both views. The DMs used harder beams (Mo/Mo 4.5%, Mo/Rh 22.4%, Rh/Rh 73.1%) while the SFMs used softer beams (Mo/Mo 44.2%, Mo/Rh 48.1%, Rh/Rh 7.8%). The peak potential used for DM was 1 to 5 kVp higher than that for SFM in 84% of cases.

Breast density on DMs generally appears to be lower than that on SFMs because of the harder beam quality used and image processing applied to the DMs. The lower density may improve the mammographic sensitivity for lesion detection on dense breasts. However, for patients with SFMs and DMs taken over time, comparison of serial mammograms for breast density changes will be problematic. We have submitted an abstract for presentation to the 89th Scientific Assembly and Annual Meeting of the Radiological Society of North America to be held in December in Chicago (ref. 3).
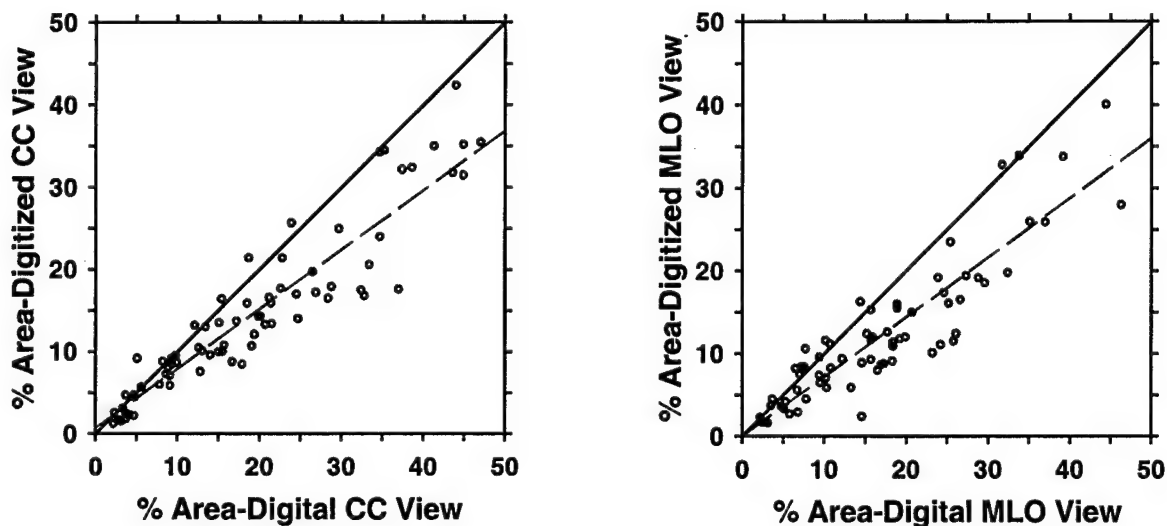

Fig. 9. Comparison of the percent mammographic density obtained on digital and digitized mammograms. Left: CC view, correlation coefficient = 0.94; Right: MLO view, correlation coefficient = 0.92. Dash line: linear regression of the data; solid line: diagonal.

(6)   Key Research Accomplishments

- Complete the collection of a data set of 67 cases of the MR images and corresponding mammograms (Task 1 and Task 3)

- Complete the analysis of the correlation between the percent volumetric fibroglandular tissue and percent mammographic dense area (Task 3).

- Complete the study and submit a journal article on the correlation between the percent volumetric fibroglandular tissue and percent mammographic dense area (Task 3).

- Continue to improve the methods for automated estimation of mammographic density on digitized screen-film mammograms (Task 2).

- Evaluate the segmentation accuracy of mammographic density by comparison with radiologists' manual segmentation (Task 2c)

- Collect a data set of full field digital mammograms with corresponding digitized screen-film mammograms (Task 1)

- Develop a Graphical User Interface (GUI) for interactive segmentation of full field direct digital mammograms (Task 4)

- Conduct study of the correlation between breast density estimated from digitized screen-film mammograms and digital mammograms (Task 2 and Task 4)

- Perform preliminary investigations of methods for automated estimation of mammographic density on digital mammograms (Task 4).

(7)   Reportable Outcomes

As a result of the support by the USAMRMC BCRP grant, we have conducted studies to investigate the correlation between mammographic density and MR volumetric fibroglandular tissue. As discussed in the progress report last year, the preliminary results were presented in the International Workshop on Digital Mammography (IWDM). The conference proceeding paper has now been published by the IWDM. This year we completed the analysis of the entire data set and prepared a manuscript based on the study. The manuscript was submitted to the Medical Physics Journal for consideration of publication.

Journal Articles:

Wei J, Chan HP, Helvie MA, Roubidoux MA, Sahiner B, Hadjiiski L, Zhou C, Paquerault S, Chenevert T, Goodsitt MM. Correlation between Mammographic Density and Volumetric Fibroglandular Tissue Estimated on Breast MR Images. Submitted to Medical Physics.

Conference Proceeding:

Chan HP, Hadjiiski LM, Roubidoux MA, Helvie MA, Paquerault S, Sahiner B, Chenevert T, Goodsitt MM. Breast density estimation: correlation of mammographic density and MR volumetric density. Proceedings of the 6th International Workshop on Digital Mammography. IWDM-2002. Bremen, Germany. June 22-25, 2002. p. 281-284.

Conference Presentation:

Chan HP, Wei, J, Zhou C, Helvie MA, Roubidoux MA, Bailey J, Hadjiiski LM, Sahiner B. Comparison of mammographic density estimated on digital mammograms and screen-film mammograms. Submitted for presentation at the 89th Scientific Assembly and Annual Meeting of the Radiological Society of North America, Chicago, IL, November 30-December 5, 2003.

(8)   Conclusions

During this project year, we have completed the analysis of the correlation between the percent mammographic dense area and the percent volumetric fibroglandular tissue measured on MR images. A semi-automatic method was developed for segmentation of the MR images and a fully automated computerized method was used to segment the mammograms. The performance of the automated density segmentation program, referred to as Mammographic Density ESTimator (MDEST), on the set of mammograms used in this study was verified with an experienced radiologist's manual segmentation. The inter-observer variability in segmentation of MR images was found to be small with correlation coefficients of 0.99. The correlation between the percent volume on MR images and percent area segmented by a radiologist for either CC view or MLO view is 0.91. The correlation between percent volume and percent area estimated by MDEST is 0.91 and 0.89, respectively, for CC and MLO views. Mammographic density is thus highly correlated with the percent volumetric fibroglandular tissue in the breast. The high correlation indicates the validity of using mammographic density as a surrogate for monitoring breast density changes. The computerized image analysis tool can provide a consistent and reproducible estimation of percent dense area on routine clinical mammograms. The automated image analysis tool may improve the sensitivity of quantifying mammographic density changes, thereby contributing to the understanding of the relationship of mammographic density to breast cancer risk, detection, and prognosis, and the prevention and treatment of breast cancer.

We have also begun the development of an automated breast density segmentation method for direct digital mammograms. We performed a study to compare breast density estimated from digitized screen-film mammograms with that estimated from digital mammograms. Our results indicate that breast density on DMs generally appears to be lower than that on SFMs because of the harder beam quality used and image processing applied to the DMs. The lower density may improve the mammographic sensitivity for lesion detection on dense breasts. However, for patients with SFMs and DMs taken over time, comparison of serial mammograms for breast density changes will be problematic. Because of the differences in the image characteristics of SFMs and DMs, the automated density segmentation program that we have developed for SFMs cannot be directly applied to DMs. We are investigating specific methods for automated segmentation of DMs. We will modify the program and evaluate its performance on DMs in the coming year.

(9) References

1. Wei J, Chan HP, Helvie MA, Roubidoux MA, Sahiner B, Hadjiiski L, Zhou C, Paquerault S, Chenevert T, Goodsitt MM. Correlation between Mammographic Density and Volumetric Fibroglandular Tissue Estimated on Breast MR Images. Submitted to Medical Physics.

2. Zhou C, Chan HP, Petrick N, Helvie MA, Goodsitt MM, Sahiner B, Hadjiiski LM. Computerized image analysis: Estimation of breast density on mammograms. Medical Physics 2001; 28: 1056-1069.

3. Chan HP, Wei, J, Zhou C, Helvie MA, Roubidoux MA, Bailey J, Hadjiiski LM, Sahiner B. Comparison of mammographic density estimated on digital mammograms and screen-film mammograms. Submitted for presentation at the 89th Scientific Assembly and Annual Meeting of the Radiological Society of North America, Chicago, IL, November 30-December 5, 2003.

(10) Appendix

Copies of the following publications are enclosed with this report:

Journal Articles:

Wei J, Chan HP, Helvie MA, Roubidoux MA, Sahiner B, Hadjiiski L, Zhou C, Paquerault S, Chenevert T, Goodsitt MM. Correlation between Mammographic Density and Volumetric Fibroglandular Tissue Estimated on Breast MR Images. Submitted to Medical Physics.

Conference Proceeding:

Chan HP, Hadjiiski LM, Roubidoux MA, Helvie MA, Paquerault S, Sahiner B, Chenevert T, Goodsitt MM. Breast density estimation: correlation of mammographic density and MR volumetric density. Proceedings of the 6th International Workshop on Digital Mammography. IWDM-2002. Bremen, Germany. June 22-25, 2002. p. 281-284.

Correlation between Mammographic Density and Volumetric Fibroglandular Tissue Estimated on Breast MR Images

Jun Wei, PhD
Heang-Ping Chan, PhD
Mark A. Helvie, MD
Marilyn A. Roubidoux, MD
Berkman Sahiner, PhD
Lubomir M. Hadjiiski, PhD
Chuan Zhou, PhD
Sophie Paquerault, PhD
Thomas Chenevert, PhD
Mitchell M. Goodsitt, PhD

Department of Radiology
University of Michigan, Ann Arbor

Correspondence :
Jun Wei, Ph.D.
Department of Radiology
University of Michigan
CGC B2103
1500 E. Medical Center Drive
Ann Arbor, MI 48109
Phone: 734-647-8553
Fax: 734-615-5513
Email: jvwei@umich.edu

1

ABSTRACT

Previous studies have found that mammographic breast density is highly correlated with breast cancer risk. Therefore, mammographic breast density may be considered as an important risk factor in studies of breast cancer treatments. In this paper, we evaluated the accuracy of using mammograms for estimating breast density by analyzing the correlation between the percent mammographic dense area and the percent glandular tissue volume as estimated from MR images. A data set of 67 cases having MR images (coronal 3D SPGR T1-weighted pre-contrast) and corresponding 4-view mammograms was used in this study. Mammographic breast density was estimated by an experienced radiologist and an automated image analysis tool, Mammography Density ESTimator (MDEST) developed previously in our laboratory. For the estimation of the percent volume of fibroglandular tissue in breast MR images, a semi-automatic method was developed to segment the fibroglandular tissue from each slice. The tissue volume was calculated by integration over all slices containing the breast. Interobserver variation was measured for 3 different readers. It was found that the correlation between every two of the three readers for segmentation of MR volumetric fibroglandular tissue was 0.99. The correlation between the percent volumetric fibroglandular tissue on MR images and the percent dense area of the CC and MLO views segmented by an experienced radiologist was both 0.91. The correlation between the percent volumetric fibroglandular tissue on MR images and the percent dense area of the CC and MLO views segmented by MDEST was 0.91 and 0.89, respectively. The root-mean-square (RMS) residual ranged from 5.4% to 6.3%. The mean bias ranged from 3% to 6%. The high correlation indicates that mammographic density can be used as a surrogate for monitoring volumetric breast density changes.

I. INTRODUCTION

Studies have shown that there is a strong positive correlation between breast parenchymal density imaged on mammograms and breast cancer risk [1-3]{ TA }. The relative risk is estimated to be about 4 to 6 for women whose mammograms have parenchymal densities over 60% of the breast area, as compared to women with less than 5% densities. Other cohort studies [4-13] also found that breast cancer risk in the category with the most extensive dense tissue was 1.8 to 6 times as high as that in the category with the least extensive dense tissue. Mammographic density as the risk indicator is greater than almost all other risk factors of breast cancer [2, 14]. Although there is no direct evidence that changes in mammographic breast densities will result in changes in breast cancer risk, the strong correlation between breast density and breast cancer risk has prompted researchers to use mammographic density for monitoring the effects of intervention as well as for studying breast cancer etiology [14-17].

A number of researchers have investigated image analysis techniques to estimate breast density [15, 18-28]. The common approaches are to analyze the textural pattern or the percentage of mammographic densities relative to the breast area. It has been found that the texture measures were correlated with parenchymal density patterns but they appeared to be less sensitive measures of relative risk than the percent dense area [1, 25, 29]. In current practice, breast density is estimated mainly by radiologists' visual judgment of the fibroglandular tissue imaged on mammograms following the Breast Imaging - Reporting and Data System (BI-RADS) lexicon [30, 31]. Because of the qualitative and subjective nature of visual judgment, there are large intraobserver and interobserver variations in the estimated breast density. The large variability may reduce the observed correlation between breast cancer risk and breast density. It may also reduce the sensitivity of studies using mammographic density for monitoring the effect of risk

3

modifying treatments. We have developed an automated image analysis system, Mammographic Density ESTimator (MDEST), to assist radiologists in estimating breast density on mammograms. Computerized analysis is expected to increase the reproducibility and consistency in the estimation of mammographic density, thereby improving the accuracy of the related studies. In our previous study, we have found that the percent mammographic density segmented by MDEST agreed closely with that estimated by radiologists' interactive thresholding [32].

The high correlation between breast cancer risk and breast density indicates that breast cancer risk may be closely related to the volume of glandular tissue in the breast. Among the modalities available for breast imaging at present, magnetic resonance (MR) imaging is likely to be the most accurate method for volumetric dense tissue estimation because fibroglandular tissue and adipose tissue can be well distinguished in MR images when a proper image acquisition technique is used [33]. However, MR imaging is expensive, making it difficult to use MR imaging as a routine monitoring tool [33, 34]. On the other hand, a mammogram is a two-dimensional (2-D) projection image of a three-dimensional (3-D) object. The area of dense tissue measured on a mammogram is not an accurate measure of the volume of fibroglandular tissue in the breast because no thickness information is used. However, mammography is a widely available low cost procedure that may be used for monitoring breast density change during preventive and interventional treatment or other studies. Women who participate in screening will also have mammograms readily available for retrospective review. Therefore, mammography will most likely be the method of choice for breast density estimation.

In this study, we investigated the correlation between the volumetric fibroglandular tissue in the breast and the projected breast dense area on mammograms by analyzing the percent

4

volumetric fibroglandular tissue in MR breast images and the percent dense area in corresponding mammograms. These comparisons will provide a better understanding of their relationship, and may lead to improved methods for utilizing mammographic density as a surrogate marker for breast cancer risk.

II. MATERIALS AND METHOD

Data Set

In a previous study, gadolinium contrast enhanced MR dynamic imaging was employed to characterize malignant and benign breast lesions. A data set was collected with IRB approval which included MR images and corresponding mammograms acquired between detection and before biopsy for a given patient. In the MR study, several series of images were acquired for each patient. Patients were scanned prone using a commercial dual phased-array breast coil. The imaging protocol included a series was the coronal 3D T1-weighted pre-contrast series (coronal sections 2-5 mm thick, 32 slices; 3D Spoiled Gradient-Recalled Echo (SPGR); TE=3.3 ms; TR=10 ms, Flip=40°, matrix=256 × 128, FOV=28-32 cm right/left, 14-16 cm superior/inferior, scan time=2 min 38 sec). This 3D SPGR sequence produces full volume coverage of both breasts with contiguous image sections. The dense parenchyma and fat tissue are well separated with this heavily T1-weighted acquisition. We used a set of 67 patients to study the correlation between the 2-D projected percentage of dense area on a mammogram and the percentage of dense tissue volume estimated from the 3-D MR images.

The mammograms consisting of the craniocaudal (CC) view and the mediolateral oblique (MLO) view of both breasts of the patient were digitized with a LUMISYS 85 laser film scanner

at a pixel size of $50\mu m \times 50\mu m$. The digitizer has a gray level resolution of 12 bits and a nominal optical density (O.D.) range of 0 to 4. For density segmentation, it is not necessary to use very high resolution images. To reduce processing time, the full resolution mammograms were first smoothed with a 16×16 box filter and subsampled by a factor of 16, resulting in $800\mu m \times 800\mu m$ images for this study.

Estimation of Fibroglandular Tissue Volume on MR Images

Since it is not our intention to routinely segment MR images for breast density estimation, we did not attempt to develop an automated method for this application. Our algorithm for segmentation of volumetric fibroglandular tissue on MR images used a semi-automatic method. The computer performed an initial segmentation. A graphical user interface (GUI) was developed to allow a user to review the segmentation of every slice and make modifications if necessary. The method consists of four steps. First, the breast boundary was detected automatically on each slice. A deformable model and manual modification were used to correct for incorrectly detected boundaries that usually occurred in slices near the chest wall where there were no well-defined breast boundaries. Because of inhomogeneity of the breast coil sensitivity, the signal intensity in the breast region was not uniform across the field of view. A background correction technique that estimated the low frequency background from the gray levels along the breast boundary was developed to reduce this systematic nonuniformity. Manual interactive thresholding of the gray level histogram in the breast region was then used to separate the fibroglandular from the fatty region. Morphological erosion was used to exclude the skin voxels along the breast boundary. Finally, the volume of fibroglandular tissue was calculated by integration over all slices containing the breast. A flow chart of our algorithm is shown in Fig. 1.

Breast Boundary Detection

6

A two-step algorithm was developed for the detection of breast boundary on each slice. First, we used a seeded pixel thresholding algorithm (SPTA) for the initial assessment of breast boundary. Second, a 2D active contour algorithm further refined the boundary. For slices close to the chest wall where no clear boundary can be seen, manual modification was used to outline an estimated boundary.

The SPTA determined the optimal threshold by iteratively partitioning the MR image into two parts and using the gradient value along the boundary of the partition as a guide in optimizing the threshold. First, the center of gravity was selected as the starting pixel on each slice. The gray level of the starting pixel was used as a threshold to create a binary partition of the image in which all pixels greater than the threshold were set to one and all other pixels were set to zero. Second, the gradient value of each pixel on the boundary of the binary partition was calculated by applying the Sobel filter to the original image. The gradient assessment for this particular binary partition was defined as the average gradient magnitude of these boundary pixels. The threshold value was reduced to zero in a stepwise manner. The partition for each threshold value was created and the gradient assessment for each partition was calculated as described above. The partition with the maximum gradient assessment was considered to be the initial segmentation result for the breast, and the boundary of this partition was considered to be the initial breast boundary.

After the initial segmentation, a deformable contour method was used to further refine the boundary. The movement of the boundary pixel was controlled by an energy function which consisted of internal energy and external energy. The internal energy components used in this study were the continuity and curvature of the contour, as well as the homogeneity of the

7

segmented partition. The external energy components were the negative of the smoothed image gradient magnitude, and a balloon force that exerted pressure at a normal direction to the contour. The energy function was defined as the following.

$$E = \sum_{c=1}^{N} [E_{int\,er}(c) + E_{exert}(c)] \tag{1}$$

where $E_{int\,er}$ and E_{exert} are the internal energy and the external energy, respectively, as defined in Eq. (2) and Eq. (3):

$$E_{int\,er} = w_{curv}E_{curv}(c) + w_{cont}E_{cont}(c) + w_{hom}E_{hom} \tag{2}$$

$$E_{exert} = w_{grad}E_{grad}(c) + w_{bal}E_{bal}(c) \tag{3}$$

where *curv, cont, grad, bal, hom* denoted curvature, continuity, gradient, balloon force and homogeneity, respectively, and each energy term was associated with a weight, *w*. The detailed definition for each term can be found in the literature [35]. An example of an MR slice of a breast is shown in Fig. 2(a). and the segmented boundary is shown in Fig. 2(b). Note that the two breasts of a patient were scanned together but each breast was analyzed separately.

Background Correction

To reduce the non-uniformity of the MR signal intensity in the breast region, a background correction technique [36] using the pixel values around the segmented breast region was employed. For a given pixel (i, j) inside the breast region, the gray value of the background image was estimated as shown in Eq. (4):

8

$$B(i,j) = \left[\frac{L}{d_l} + \frac{R}{d_r} + \frac{U}{d_u} + \frac{D}{d_d} \right] \bigg/ \left[\frac{1}{d_l} + \frac{1}{d_r} + \frac{1}{d_u} + \frac{1}{d_d} \right] \qquad (4)$$

where L, R, U and D are the average gray values inside a breast background estimation region (BBER) centered at the left, right, upper and lower pixels on the breast boundary, respectively. A BBER was defined as the intersection of a 21×21-pixel box and the breast region. The center pixels for the left and right boxes were the intersection points between the breast boundary and a horizontal line passing through the given pixel (i, j). Similarly, the upper and lower center pixels for the upper and lower boxes were the intersection points between the breast boundary and a vertical line passing through the given pixel (i, j). Only the pixels that were within the intersected area between the 21×21-pixel box and the breast region were included in the definition of the BBER and the calculation of the average gray value. The contributions of the average gray levels to the background pixel (i, j) were inversely weighted by their distances d_l, d_r, d_u, d_d from the given pixel (i, j). An example of the background corrected image is shown in Fig. 2(c).

Segmentation of Fibroglandular Tissue

We developed a GUI that allowed the user to perform a combination of manual and automatic operations to segment the breast boundary and the fibroglandular tissue on the MR images. The first window (not shown) displayed the MR series and the corresponding mammogram of each breast to give the user an overview of the breast. The segmentation of the fibroglandular tissue on each MR slice was processed in the second window, shown in Fig. 3. The original MR slice, the corresponding background corrected image, and the segmented binary

image were shown in the upper part of the window. At the lower part of the window, the histogram of the voxel values in the breast region was shown. The user performed interactive thresholding on the histogram and the segmented binary image corresponding to the chosen threshold was displayed in real time in the upper part. If the breast boundary, which was automatically segmented by the computer initially, had to be corrected, the user could go to the third window and manually move the apices of the polygon outlining the boundary. The voxels contributed by the nipple were excluded. On the slices containing breast skin that had voxel values similar to those of fibroglandular tissue, a morphological erosion operation was applied to the breast boundary to exclude the skin voxels from the calculation of the fibroglandular tissue volume in the slice. The size of the structuring element could be selected interactively on the fourth window and the eroded boundary was displayed instantly for a chosen erosion operation. The user might again change the structuring element if the erosion result of the previous choice was deemed unsatisfactory. Since the eroded boundary only marked the region within which the fibroglandular voxels would be summed and would not be used for the calculation of the breast volume, as described below, it did not need to be precise as long as it excluded the skin voxels while not excluding the fibroglandular voxels.

MR Fibroglandular Tissue Volume

After the fibroglandular tissue was segmented for each slice, the total number of voxels containing the fibroglandular tissue was obtained as a summation of these voxels over all slices of the breast. The total volume of the breast was obtained as the summation of the voxels enclosed by the breast boundary before morphological erosion. The ratio of these two volumes provided the percent volumetric fibroglandular tissue in the breast.

Mammographic Density Segmentation

10

We have previously developed an automated method for segmentation of the dense fibroglandular area on mammograms. The method, referred to as the Mammographic Density ESTimator (MDEST) was described in detail elsewhere [32]. In brief, the breast boundary on the digitized mammogram is tracked. A dynamic-range compression technique reduces the gray level range of the breast area. By analyzing the shape of the gray level histogram, a rule-based classifier classifies the breast density into one of four classes. Typically, a Class I breast is almost entirely fat, it has a single narrow peak on the histogram. A Class II breast contains scattered fibroglandular densities. Its histogram has two main peaks, with the smaller peak on the right of the bigger one. A Class III breast is heterogeneously dense. Its histogram also has two peaks, but the smaller peak is on the left of the bigger one. A Class IV breast is extremely dense. Its histogram has mainly a single dominant peak, but the peak is wider compared with the peak in the Class I histogram. A second smaller peak sometimes occurs on the left of the main peak. Based on the histogram shape, a threshold is automatically calculated to separate the dense and fatty pixels. The mammographic density was estimated as the percentage of fibroglandular tissue area relative to the total breast area. For MLO view mammograms, the pectoral muscle is detected and excluded from the density area or breast area calculations. In our previous work, the performance of MDEST was verified by comparison with manual segmentation by 5 breast imaging radiologists using a data set of 260 mammograms from 65 patients that were different from the cases used in the current study. We found that the correlation between the computer-estimated percent dense area and the average segmentation by the 5 radiologists was 0.94 and 0.91, respectively, for CC and MLO views, with a mean bias of less than 2%.

MDEST was applied to the mammograms of the 67 patients used in this study. The percent dense area on mammograms was estimated for the CC-view and the MLO-view mammogram of each breast separately. In addition, an MQSA-qualified radiologist also

11

segmented the dense area by interactive thresholding for each mammogram. The correlation between the mammographic density obtained by manual and automatic segmentation is shown in Fig. 4(a) and 4(b) for the CC view and MLO view, respectively. The correlation coefficients for the CC view and MLO view were both 0.91. The mammographic densities estimated by automatic and manual segmentation were compared with the percent volumetric fibroglandular tissue on MR images as described below.

Observer Experiments

We performed observer experiments to evaluate the inter-observer variations in the segmentation of fibroglandular tissue using the semi-automatic method. Twenty-three MR cases from the data set were randomly selected for this observer experiment. There were a total of 41 breasts because some cases had only one breast. Two MQSA-qualified radiologists performed the segmentation of the fibroglandular tissue on MR images using the semi-automatic method implemented with the GUI. A Ph. D. researcher who was trained by these radiologists also performed the segmentation independently with the GUI.

After verifying the consistency of segmentation by these observers, the trained Ph.D. completed the segmentation of all MR cases. The correlation between percent volumetric fibroglandular tissue on MR images and percent dense area on mammograms was then examined for the entire data set.

III. RESULTS

Inter-observer variation between radiologists

Fig. 5 shows the comparison of the percent volumetric fibroglandular tissues on MR images segmented by two radiologists for the 41 breasts. The correlation between the segmentation results of the two radiologists is 0.99. To compare the difference between their results, the mean difference and the root-mean-square (RMS) residual, which is the residual from the linear least-squares-fitted line, was also calculated. The mean difference was found to be 0.7 and the RMS residual was 1.4.

Inter-observer variation between radiologists and trained Ph. D.

Fig. 6 showed the comparison of the percent volumetric fibroglandular tissues segmented by the trained Ph. D. against those segmented by the two radiologists. The correlation between the result of the trained Ph. D. and the results of both radiologists was 0.99. The corresponding mean differences were 0.8 and 0.5, respectively, and the RMS residuals were 1.2 and 0.5, respectively.

Correlation betweeen percent volumetric fibroglandular tissue on MR images and percent mammographic density

The percent volumetric fibroglandular tissue on MR images was compared with the percent dense area on CC- and MLO-view mammograms. After verifying that the difference in segmentation between the trained Ph. D. and the radiologists was similar to the interobserver variations between the two experienced radiologists, the trained Ph. D. completed the segmentation of the entire data set.

Fig. 7 shows the comparison of the percent volumetric fibroglandular tissue on MRI and the percent mammographic density segmented by a radiologist. The percent areas on CC- and MLO-view mammograms are higher than the percent volume on MR images by 5.7% and 3.0%,

13

respectively.

Fig. 8 shows the comparison of the percent volumetric fibroglandular tissue on MRI and the percent mammographic density segmented by MDEST. The percent areas on CC- and MLO-view mammograms segmented by the computer are higher than the percent volume on MR images by 5.2% and 2.6%, respectively.

The correlation coefficients, the mean differences, and the RMS residuals between the percent volumetric fibroglandular tissue on MR images and percent dense area on mammograms are compared in Table. 1. The correlation between the percent volume on MR images and percent area on mammograms of the fibroglandular breast tissue is high, ranging from 0.89 to 0.91. Although it is not expected that the values of percent volume agree with the values of percent area, their mean differences range only from 3% to 6%.

IV. DISCUSSION

Our purpose in this paper was to investigate the relationship between the percent dense area on mammogram and the percent fibroglandular tissue volume on MR image. We found a direct correlation between mammographic density and MR volumetric density (Fig. 7 and Fig. 8). The correlation coefficients between the percent area on mammogram and the percent volume on MR images are high at 0.89 and 0.91. These results are more promising that those found in previous studies that attempted to correlate percent dense area on mammograms with MR information. Graham et al. [33] investigated the relationship between percent density (projected dense area) on mammogram and two objective MR parameters of breast tissue, relative water content and mean T2 relaxation. Their results with 45 cases showed a positive correlation

14

between percent density and relative water content (Pearson correlation coefficient = 0.79) and a negative correlation between percent density and mean T2 value (Pearson correlation coefficient = -0.61). Another study by Lee et al [34] analyzed fatty and fibroglandular tissue in different age groups to compare x-ray mammography with T1 weighted MR images. Their study with 40 cases indicated that the correlation between the two techniques is 0.63 when the fat content was more than 45%. However, the correlation coefficient decreased to 0.34 when their analysis included only dense breasts.

It may be noted that although MR imaging is currently the most accurate method for estimating the volumetric fibroglandular tissue in the breast, it is still not the ideal tool. Fibrous tissue and glandular tissue are not well separated with current MR imaging techniques. Since the amount of glandular tissue in the breast is the important factor relating to breast cancer risk, further studies are warranted for differentiating the glandular and the fibrous components of the imaged volume. The correlation between the percent glandular tissue volume and percent projected dense area on mammogram will be a more reliable indicator of the usefulness of mammographic density analysis.

The density on mammograms is a 2D projected area of the fibroglandular tissues. The percent dense area is not expected to be equal in value to the percent volume. The average differences between the percent volume and the percent area on CC and MLO views, as determined by the radiologist's interactive segmentation, are 5.7 and 3.0, respectively (Table I), with the percent dense area values being higher. We also investigated the RMS residual between the percent volume and the percent area when the relationship between them was assumed to be linear. The RMS residual between the percent volume and the percent area on CC and MLO views are 6.3 and 5.6, respectively (Table I), relative to the straight line obtained from linear

least squares fits to the data. One possible factor that may contribute to a higher value of percent dense area on mammograms than the percent volume value on MR images is that the tissue volume imaged by the two modalities is somewhat different. The MR images include more tissue near the chest wall, which is mainly retroglandular adipose tissue, than a mammogram does, thus reducing the percent fibroglandular tissue volume.

Geometrically, we do not expect the relationship between volume and its projected 2D area to be linear. In a hypothetical situation such that the dense tissue volume is a sphere (volume $= \frac{4}{3}\pi r^3$) enclosed inside a concentric spherical shell of fatty tissue volume, the percent projected 2D area (area $= \pi r^2$) of the inner sphere relative to the outer sphere is equal to the percent volume to the power of 2/3. The relationship between the percent area and the percent volume is therefore not linear, and the percent area is larger in value than the percent volume for any ratio of radii between the two spheres. In general, the compressed breast and the dense tissue are not spherical. To investigate the empirical relationship between the percent area and the percent volume in the nonlinear situation, we applied least squares fits in several polynomial models to the data points in Fig. 7. The results are shown in Table 2 and Fig. 9. Comparison of Table 1 and Table 2 indicates that the $Y = kx^{2/3}$ model, (x=percent fibroglandular tissue volume, Y=percent mammographic dense area) resulted in slightly larger RMS residuals than the linear model. The model $Y = kx^m$ with m equal to 0.83 and 0.86, respectively, for CC and MLO views slightly reduced the RMS residuals. The best fit was obtained from the model $Y = k_1 x^m + k_2$. However, the situation that the percent projected area was negative when the percent volume was zero would not occur physically. Note that if the model was fitted to the percent area data segmented by MDEST (Fig. 8), the k_2 values would become positive, indicating that the non-zero k_2 values are likely caused by segmentation biases.

16

Overall, these models demonstrate that there is no simple mathematical relationship between the percent volume and the percent projected area but the values for the exponents appeared to be in a reasonable range. The relationship between the percent volume of two 3D objects, one within another, and their percent projected 2D area depends on their shapes. For example, the closer the two volumes are to concentric cylinders of the same height, the closer the exponent is to unity. The spread of the data points can therefore be attributed to the various irregular shapes of the fibroglandular tissue in the breasts, the changes in the shapes of the fatty and fibroglandular tissue due to compression, as well as the uncertainties in segmentation of both the mammograms and the MR images. Nevertheless, the strong correlation observed between the percent dense area on mammograms and the percent volumetric fibroglandular tissue on MR images indicates that mammographic density can be used as a surrogate for percent fibroglandular tissue volume for monitoring changes in breast density.

Recently, some researchers attempted to estimate the thickness of the fibroglandular tissue in local regions of the mammograms from the projected density [37]. This approach is expected to provide a more accurate estimation of the fibroglandular tissue volume if the true thicknesses of the fibroglandular tissue and fatty tissue can be determined at various locations of the projected breast region. The volume of the fibroglandular tissue can then be summed over the pixels in the breast region and the percent volume calculated. However, to obtain accurate measurements, this approach requires the knowledge of the sensitometric curve for the screen-film mammogram at the imaging facility (or use of a digital detector with linear response) and other physical parameters such as the scatter fraction, the beam quality and beam hardening, in addition to the compressed breast thickness and the breast shape profile at the periphery. Some of the requirements may be circumvented by using a look-up table predetermined with phantom calibration. Other factors may have to be approximated or ignored, or require further corrections

17

by imaging each mammogram with a calibration phantom placed adjacent to the breast. This method is still being developed and the accuracy of estimating the thickness of the local fibroglandular tissue from a mammogram is yet to be determined. To our knowledge, no study to date has demonstrated that fibroglandular tissue volume estimated from mammograms has a higher correlation with the percent volumetric fibroglandular tissue volume estimated from MR images or other volumetric methods than we found in our current study. Furthermore, even if the local fibroglandular tissue thickness on mammograms can be measured in a laboratory or in an academic center using elaborate calibration schemes, it is doubtful that these methods can be translated into routine clinical measurement in mammography clinics. Its use may then be limited to controlled clinical trials. Estimation of the percent dense area projected on mammograms is likely a more practical approach for breast density assessment. The high correlation between the percent dense area and the percent fibroglandular tissue volume on MR images as demonstrated in the current study further supports the validity of this approach.

V. Conclusion

In this study, we investigated the correlation between the percent mammographic dense area and the percent volumetric fibroglandular tissue as measured on MR images. A semi-automatic method was developed for segmentation of the MR images and a fully automated computerized method, MDEST, was used to segment the mammograms. The performance of MDEST on the set of mammograms used in this study was verified with an experienced radiologist's manual segmentation. The inter-observer variability in segmentation of MR images was found to be small with correlation coefficients of 0.99. The correlation between the percent volume on MR images and percent area segmented by a radiologist for either CC view or MLO view is 0.91. The correlation between percent volume and percent area estimated by MDEST is

0.91 and 0.89, respectively, for CC and MLO views. Mammographic density is thus highly correlated with the percent volumetric fibroglandular tissue in the breast. The high correlation indicates the validity of using mammographic density as a surrogate for monitoring breast density changes. Our computerized image analysis tool, MDEST, can provide a consistent and reproducible estimation of percent dense area on routine clinical mammograms. The automated image analysis tool may improve the sensitivity of quantifying mammographic density changes, thereby contributing to the understanding of the relationship of mammographic density to breast cancer risk, detection, and prognosis, and the prevention and treatment of breast cancer.

REFERENCE

[1] A. F. Saftlas, R. N. Hoover, L. A. Brinton, M. Szklo, D. R. Olson, M. Salane, and J. N. Wolfe, "Mammographic densities and risk of breast cancer," Cancer 67, 2833-2838 (1991).

[2] N. F. Boyd, G. A. Lockwood, J. W. Byng, D. L. Tritchler, and M. J. Yaffe, "Mammographic densities and breast cancer risk," Cancer Epidemiology Biomarkers & Prevention 7, 1133-1144 (1998).

[3] C. M. Vachon, C. C. Kuni, K. Anderson, V. E. Anderson, and T. A. Sellers, "Association of mammographically defined percent breast density with epidemiologic risk factors for breast cancer (United States)," Cancer Causes & Control 11, 653-662 (2000).

[4] P. M. Krook, "Mammographic parenchymal patterns as risk indicators for incident cancer in a screening program: an extended analysis," Amer. J. Roentgenology 131, 1031-1035 (1978).

[5] R. L. Egan and R. C. Mosteller, "Breast cancer mammography patterns," Cancer 40, 2087-2090 (1977).

[6] B. Threatt, J. M. Norbeck, N. S. Ullman, R. Kummer, and P. Roselle, "Association between mammographic parenchymal pattern classification and incidence of breast cancer," Cancer 45, 2550-2556 (1980).

[7] M. Moskowitz, P. Gartside, and C. Mclaughlin, "Mammographic patterns as markers for high-risk benign breast disease and incident cancers," Radiology 134, 293-295 (1980).

20

[8]I. Witt, H. S. Hansen, and S. Brunner, "The risk of developing breast cancer in relation to mammography findings," European Radiology 4, 65-67 (1984).

[9]S. Ciatto and M. Zappa, "A prospective study of the value of mammographic pattern as indicators of breast cancer risk in a screening experience," European Radiology 17, 122-125 (1993).

[10]E. Thurfjell, C. C. Hsieh, L. Lipworth, A. Ekbom, H. O. Adami, and D. Trichopoulos, "Breast size and mammographic pattern in relation to breast cancer risk," European Journal of Cancer Prevention 5, 37-41 (1996).

[11]I. Kato, C. Beinart, A. Bleich, S. Su, M. Kim, and P. G. Toniolo, "A nested case-control study of mammographic patterns, breast volume and breast cancer (New York City, NY, United States)," Cancer Causes & Control 6, 431-438 (1995).

[12]E. Sala, R. Warren, J. McCann, S. Duffy, N. Day, and R. Luben, "Mammographic parenchymal patterns and mode of detection: implications for the breast screening programme," Journal of Medical Screening 5, 207-212 (1998).

[13]T. M. Salminen, I. E. Saarenmaa, M. M. Heikkila, and M. Hakama, "Is a dense mammographic parenchymal pattern a contraindication to hormonal replacement therapy?," Acta Oncologica 39, 969-972 (2000).

[14]C. Byrne, C. Schairer, J. N. Wolfe, N. Parekh, M. Salane, L. A. Brinton, R. Hoover, and R. Haile, "Mammographic features and breast cancer risk: Effects with time, age, and menopause status," J. Natl. Cancer Inst. 87, 1622-1629 (1995).

[15]N. F. Boyd, C. Greenberg, G. Lockwood, L. Little, L. Martin, J. Byng, Y. Martin, and D. Tritchler, "Effects at two years of a low-fat, high--carbohydrate diet on radiologic features of the breast: Results from a randomized trial," J. Natl. Cancer Inst. 89, 488-467 (1997).

[16]D. V. Spicer, G. Ursin, Y. R. Parisky, J. G. Pearce, D. Shoupe, A. Pike, and M. C. Pike, "Changes in mammographic densities induced by a hormonal contraceptive designed to reduce breast cancer risk," J. Natl. Cancer Inst. 86, 431-436 (1994).

[17]J. Brisson, R. Verreault, A. S. Morrison, D. Tennina, and F. Meyer, "Diet, mammographic features of breast tissue, and breast cancer risk," Am. J. Epidemiology 130, 14-24 (1989).

[18]J. N. Wolfe, "Mammography: Ducts as a sole indicator of breast carcinoma," Radiology 89, 206-210 (1967).

[19]J. N. Wolfe, "The prominent duct pattern as an indicator of cancer risk," Oncology 23, 149-158 (1969).

[20]J. N. Wolfe, "Breast patterns as an index of risk for developing breast cancer," Am. J. Roentgenol. 126, 1130-1139 (1976).

[21]J. N. Wolfe, "Risk for breast cancer development determined by mammographic parenchymal pattern," Cancer 37, 2486-2492 (1976).

[22]I. E. Magnin, F. Cluzeau, C. L. Odet, and A. Bremond, "Mammographic texture analysis: An evaluation of risk for developing breast cancer," Opt Eng 25, 780-784 (1986).

[23]J. W. Byng, N. F. Boyd, E. Fishell, R. A. Jong, and M. J. Yaffe, "Automated analysis of mammographic densities," Phys Med Biol 41, 909-923 (1996).

[24]J. W. Byng, N. F. Boyd, E. Fishell, R. A. Jong, and M. J. Yaffe, "The quantitative-analysis of mammographic densities," Phys. Med. Biol. 39, 1629-1638 (1994).

[25]M. J. Yaffe, N. F. Boyd, J. W. Byng, R. A. Jong, R. Fishell, G. A. Lockwood, L. E. Little, and D. L. Tritchler, "Breast cancer risk and measured mammographic density," European J. of Cancer Prevention 7, Suppl. 1, S47-S55 (1998).

[26]Z. Huo, M. L. Giger, D. E. Wolverton, and W. Zhong, "Computerized analysis of mammographic parenchymal patterns for breast cancer risk assessment: Feature selection," Medical Physics 27, 4-12 (2000).

[27]J. J. Heine and R. P. Velthuizen, "A statistical methodology for mammographic density detection," Medical Physics 27, 2644-2651 (2000).

[28]J. M. Boone, K. K. Lindfors, C. S. Veatty, and J. A. Seibert, "A breast density index for digital

mammograms based on radiologists' ranking," J. Digital Imaging 11, 101-115 (1998).

[29]J. N. Wolfe, A. F. Saftlas, and M. Salene, "Evaluation of mammographic densities: A case-control study," AJR 148, 1087-1092 (1987).

[30]*American College of Radiology. Breast Imaging - Reporting and Data System (BI-RADS)*, Third Edition ed. (American College of Radiology, Reston, VA, 1998).

[31]E. White, P. Velentgas, M. T. Mandelson, C. D. Lehman, J. G. Elmore, P. Porter, Y. Yasui, and S. H. Taplin, "Variation in mammographic breast density by time in menstrual cycle among women aged 40-49 years," J. Natl. Cancer Inst. 90, 906-910 (1998).

[32]C. Zhou, H. P. Chan, N. Petrick, M. A. Helvie, M. M. Goodsitt, B. Sahiner, and L. M. Hadjiiski, "Computerized image analysis: Estimation of breast density on mammograms," Medical Physics 28, 1056-1069 (2001).

[33]S. J. Graham, M. J. Bronskill, J. W. Byng, M. J. Yaffe, and N. F. Boyd, "Quantitative correlation of breast tissue parameters using magnetic resonance and x-ray mammography," British J Cancer 73, 162-168 (1996).

[34]N. A. Lee, H. Rusinek, J. Weinreb, R. Chandra, H. Toth, C. Singer, and G. Newstead, "Fatty and fibroglandular tissue volumes in the breasts of women 20-83 years old: comparison of x-ray mammography and computer-assisted MR imaging," American Journal of Roentgenology 168, 501-506 (1997).

[35]B. Sahiner, N. Petrick, H. P. Chan, L. M. Hadjiiski, C. Paramagul, M. A. Helvie, and M. N. Gurcan, "Computer-Aided Characterization of Mammographic Masses: Accuracy of Mass Segmentation and its Effects on Characterization," IEEE Transactions on Medical Imaging 20, 1275-1284 (2001).

[36]B. Sahiner, H. P. Chan, N. Petrick, D. Wei, M. A. Helvie, D. D. Adler, and M. M. Goodsitt, "Classification of mass and normal breast tissue: A convolution neural network classifier with spatial domain and texture images," IEEE Transactions on Medical Imaging 15, 598-610 (1996).

[37]O. Pawluczyk, B. J. Augustine, M. J. Yaffe, D. Rico, J. Yang, G. E. Mawdsley, and N. F. Boyd, "A volumetric method for estimation of breast density on digitized screen-film mammograms," Medical Physics 30, 352-364 (2003).

Table 1. Statistic analysis of the relationship between percent fibroglandular tissue volume on breast MR images and percent dense area on mammograms segmented by radiologist and MDEST.

	Radiologist		Computer (MDEST)	
	CC vs MRI	MLO vs MRI	CC vs MRI	MLO vs MRI
Correl. Coeff.	0.91	0.91	0.91	0.89
RMS Residual	6.3	5.6	5.8	5.4
Mean Diff.	5.7	3.0	5.2	2.6

Table 2. Analysis of the relationship between percent fibroglandular tissue volume (x) on breast MR images and percent dense area (Y) on mammograms segmented by radiologist using three mathematical models. m, k, k_1 and k_2 are constants determined by least squares curve fitting.

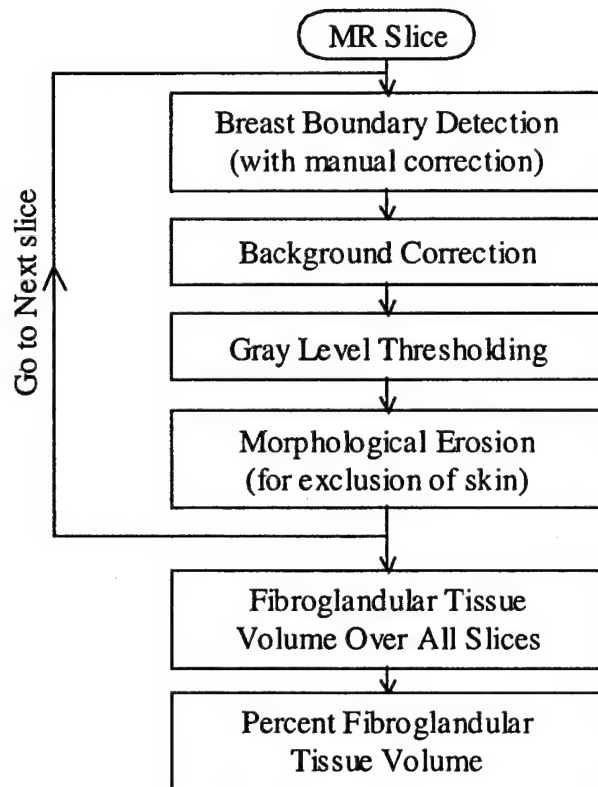| Mathematical Model		$Y = kx^{2/3}$	$Y = kx^m$	$Y = k_1x^m + k_2$
CC vs MRI	Least Squares Fit	$Y = 0.82x^{2/3}$	$Y = 1.03x^{0.83}$	$Y = 1.02x^{0.48} - 0.19$
	RMS Residual	6.5	6.0	5.6
	Coefficient of determination	0.82	0.85	0.87
MLO vs MRI	Least Squares Fit	$Y = 0.73x^{2/3}$	$Y = 0.96x^{0.86}$	$Y = 0.90x^{0.60} - 0.09$
	RMS Residual	6.0	5.5	5.3
	Coefficient of determination	0.80	0.84	0.85

Fig. 1. The flow-chart for the segmentation of the fibroglandular tissue on MR images.
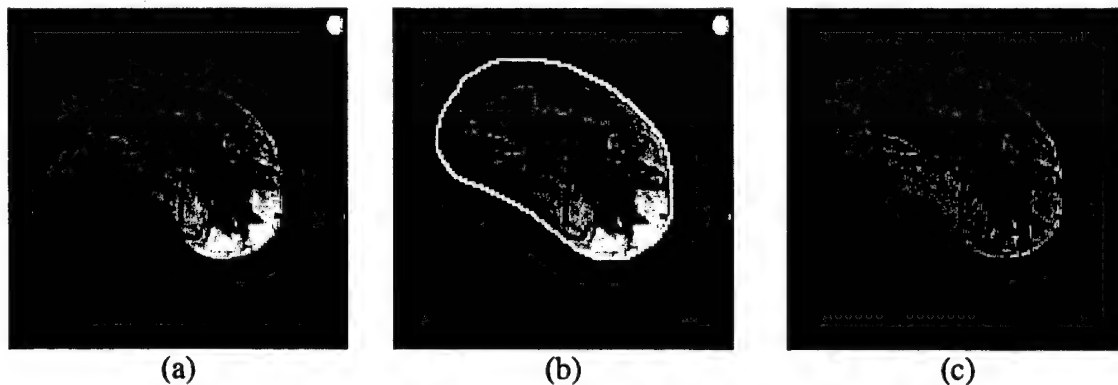
Fig. 2. An example of the first three processing blocks in Fig. 1. (a) original MR slice, (b) automatically-detected breast boundary superimposed on image, and (c) background-corrected image.
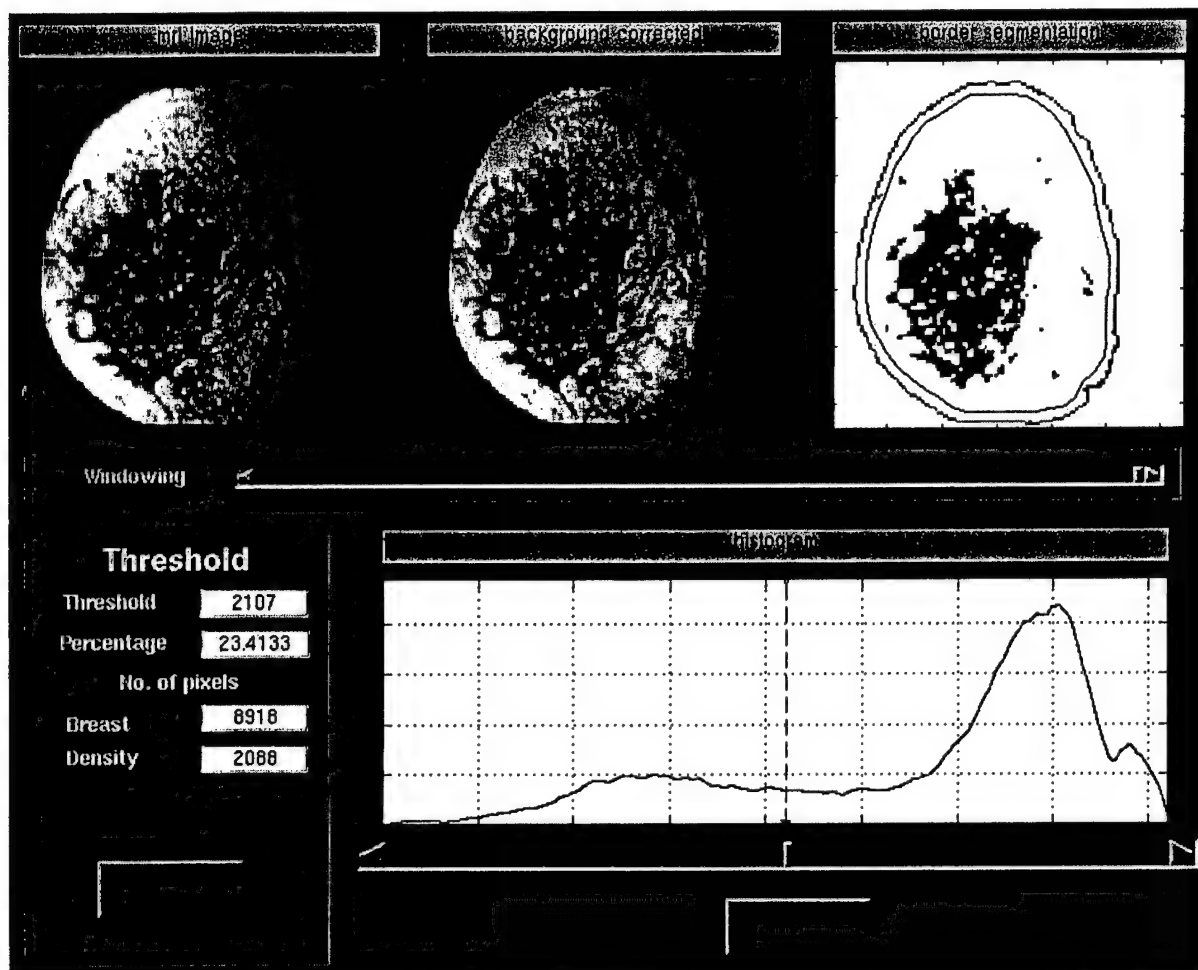
Fig. 3. The graphic user interface for the segmentation of the fibroglandular tissues on MR slice. The upper row shows the original MR slice (left), the background-corrected image (middle) and the segmented binary image (right). The segmented image responds to the reader's adjustment of the gray level threshold (lower row) in real time so that the reader can choose the appropriate threshold by inspecting the segmented image visually. The dark area in the segmented image indicates the fibroglandular tissue and the white area indicates the adipose tissue. The inner line along the breast boundary is the boundary obtained by morphological erosion to exclude the skin voxels for calculating the fibroglandular tissue volume.
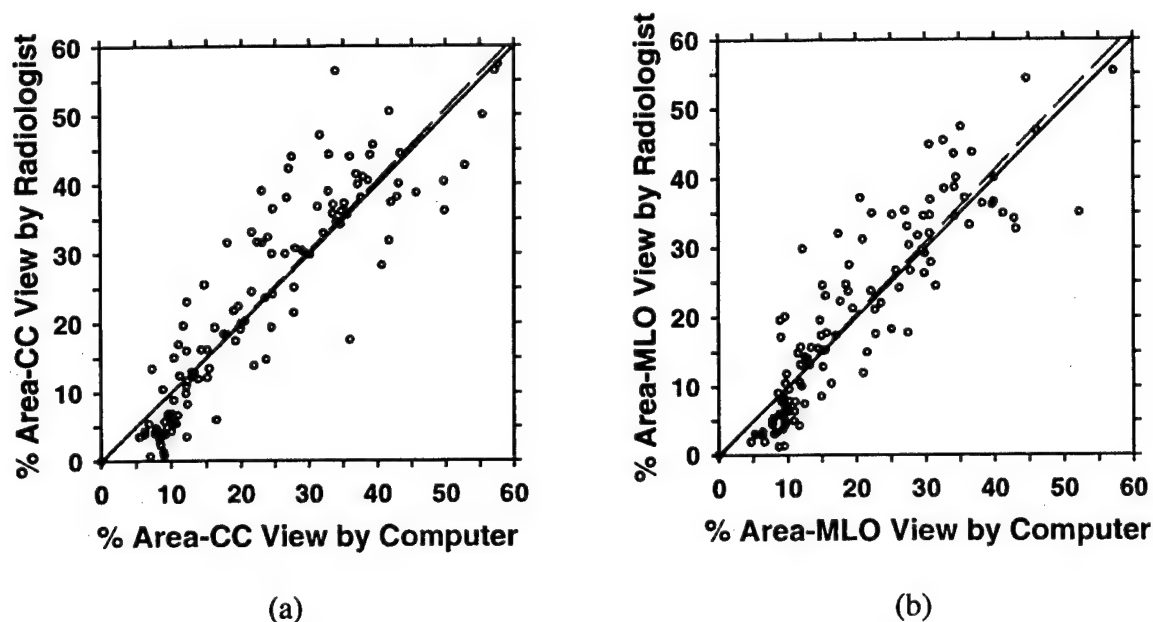
Fig. 4. Comparison of the percent mammographic density obtained from interactive thresholding by an MQSA-qualified radiologist and that estimated by our automated MDEST computer program. (a) CC view, correlation coefficient = 0.91 (b) MLO view, correlation coefficient = 0.91. Dash line: linear regression of the data; solid line: diagonal.
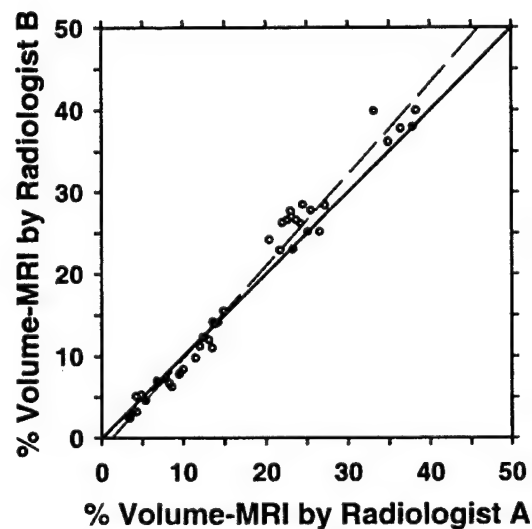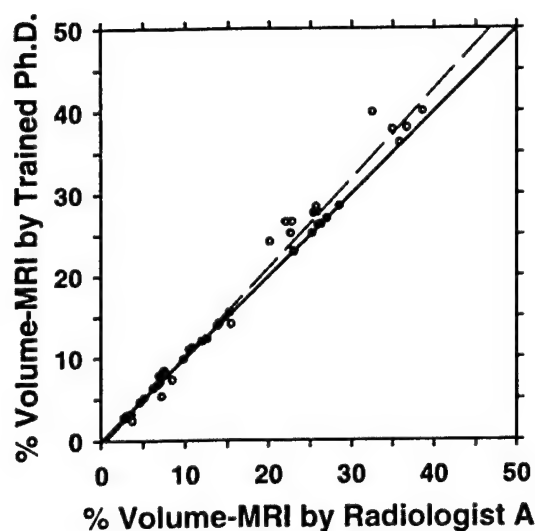
Fig. 5. Comparison of the segmentation of fibroglandular tissue from MR images between two experienced MQSA-qualified radiologists, correlation coefficient = 0.99. Dash line: linear regression of the data; solid line: diagonal.

Fig. 6. Comparison of the segmentation of fibroglandular tissue from MR images between the trained Ph. D. and two experienced MQSA-qualified radiologists. (a) Radiologist A, correlation coefficient = 0.99, (b) Radiologist B, correlation coefficient = 0.99. Dash line: linear regression of the data; solid line: diagonal.

Fig. 7. Comparison of the percent fibroglandular tissue volume on MR images and the percent dense area on mammograms segmented by an experienced radiologist. (a) CC view, correlation coefficient = 0.91, (b) MLO view, correlation coefficient = 0.91. Dash line: linear regression of the data; solid line: diagonal.

Fig. 8. Comparison of the percent volume on MR images and the percent area on mammogram segmented by our automated MDEST computer program. (a) CC view, correlation coefficient = 0.91, (b) MLO view, correlation coefficient = 0.89. Dash line: linear regression of the data; solid line: diagonal.

Fig. 9. Nonlinear fitting of the relationship between the percent volume and the percent area segmented by radiologist with least squares method. (a) CC view, (b) MLO view. Dash line: $y = kx^{2/3}$; dash-dot-dot line: $y = kx^{m}$; solid line: $y = k_1 x^{m} + k_2$. The fitted parameters of the models, m, k, k_1 and k_2, are shown in Table 2.

Fig. 1   The flow-chart for the segmentation of the fibroglandular tissue on MR images.

(a)   (b)   (c)

Fig. 2   An example of the first three processing blocks in Fig. 1. (a) original MR slice, (b) automatically-detected breast boundary superimposed on image, and (c) background-corrected image.

29

Fig. 3 The graphic user interface for the segmentation of the fibroglandular tissues on MR slice. The upper row shows the original MR slice (left), the background-corrected image (middle) and the segmented binary image (right). The segmented image responds to the reader's adjustment of the gray level threshold (lower row) in real time so that the reader can choose the appropriate threshold by inspecting the segmented image visually. The dark area in the segmented image indicates the fibroglandular tissue and the white area indicates the adipose tissue. The inner line along the breast boundary is the boundary obtained by morphological erosion to exclude the skin voxels for calculating the fibroglandular tissue volume.

(a)   (b)

Fig. 4   Comparison of the percent mammographic density obtained from interactive thresholding by an MQSA-qualified radiologist and that estimated by our automated MDEST computer program. (a) CC view, correlation coefficient = 0.91 (b) MLO view, correlation coefficient = 0.91. Dash line: linear regression of the data; solid line: diagonal.

Fig. 5 Comparison of the segmentation of fibroglandular tissue from MR images between two experienced MQSA-qualified radiologists, correlation coefficient = 0.99. Dash line: linear regression of the data; solid line: diagonal.

Fig. 6 Comparison of the segmentation of fibroglandular tissue from MR images between the trained Ph. D. and two experienced MQSA-qualified radiologists. (a) Radiologist A, correlation coefficient = 0.99, (b) Radiologist B, correlation coefficient = 0.99. Dash line: linear regression of the data; solid line: diagonal.
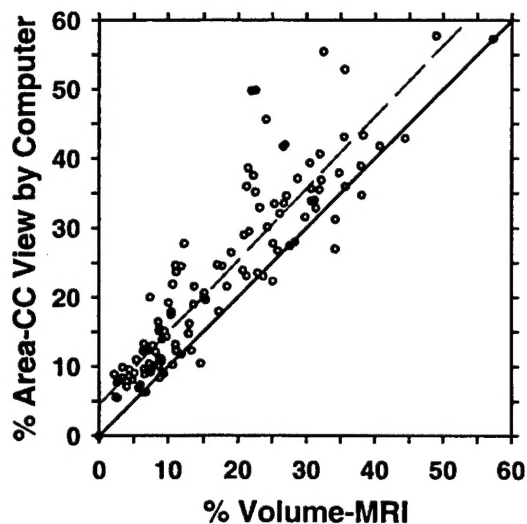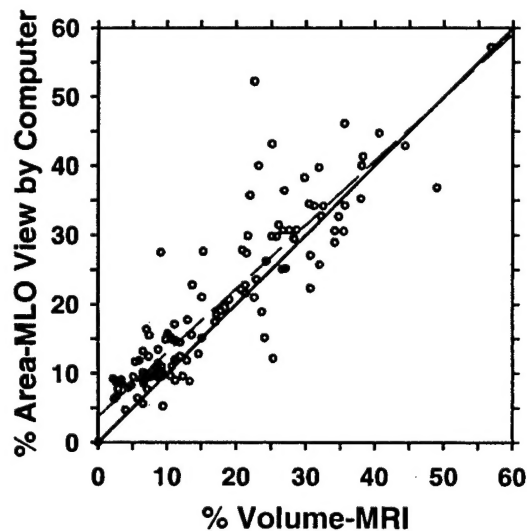

Fig. 7 Comparison of the percent fibroglandular tissue volume on MR images and the percent dense area on mammograms segmented by an experienced radiologist. (a) CC view, correlation coefficient = 0.91, (b) MLO view, correlation coefficient = 0.91. Dash line: linear regression of the data; solid line: diagonal.
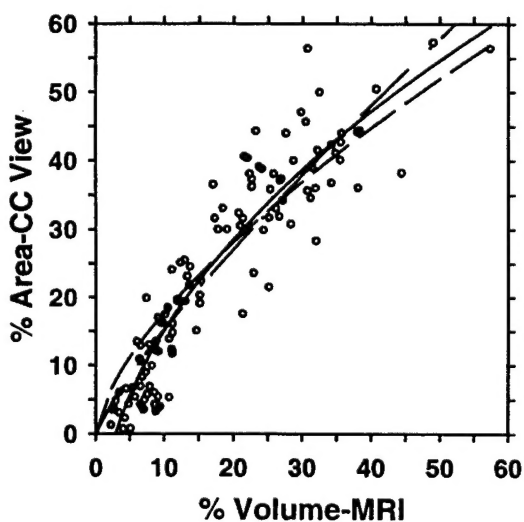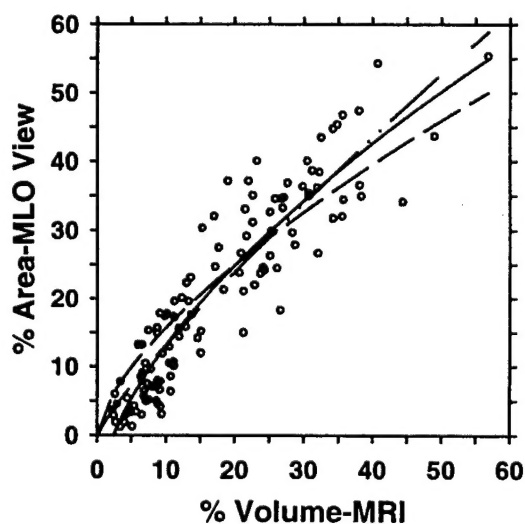
Fig. 8 Comparison of the percent volume on MR images and the percent area on mammogram segmented by our automated MDEST computer program. (a) CC view, correlation coefficient = 0.91, (b) MLO view, correlation coefficient = 0.89. Dash line: linear regression of the data; solid line: diagonal.

Fig. 9 Nonlinear fitting of the relationship between the percent volume and the percent area segmented by radiologist with least squares method. (a) CC view, (b) MLO view. Dash line: $y = kx^{2/3}$; dash-dot-dot line: $y = kx^m$; solid line: $y = k_1 x^m + k_2$. The fitted parameters of the models, m, k, k_1 and k_2, are shown in Table 2.

4. Conclusions

We conclude from our study that computer-placed prompts have no impact on sensitivity and specificity with different groups of film reader working within the NHSBSP. Furthermore, there is no difference in time taken to read films between different professional groups of reader and again, this is not affected by the use of computer-placed prompts. Our hypothesis that CAD would be of greater use to radiographers is not supported.

We are considering a new test set of cases that are subtle but prompted by CAD. In these cases there is more scope for detecting improvements due to the computer prompts. It may be that this test set will also reveal some differences in performance between the professional groups.

References

1. Forrest A, P, M, Breast Cancer Screening: Report to the Health Ministers of England, Wales, Scotland and Northern Ireland. HMSO, London, 1986.
2. NHSBSP. http://www.cancerscreening.nhs.uk/breastscreen/research.html (accessed on 12/4/2002)
3. Department of Health. http://www.doh.gov.uk/cancer/cancerplan.htm (accessed on 12/4/2002)
4. Field S. UK Radiologist Workforce Survey - Breast Imaging Service. *Royal College of Radiologists Newsletter* 1998; 54: 12-4
5. Chan H, Doi K, Vyborny C et al. Improvements in radiologists' detection of clustered microcalcifications in mammograms. The potential of computer-aided diagnosis. *Invest Radiol* 1990 25: 1102.
6. Hutt I, Astley S and Boggis C Prompting as an aid to diagnosis in mammography. In Gale A, Astley S, Dance D and Cairns A(eds.) *Digital Mammography* Elsevier, 1994 pp: 389
7. Nishikawa R N, Wolverton D E, Schmidt R A et al. Radiologists' ability to discriminate computer-detected true and false positives from an automated scheme for the detection of clustered micro-calcifications on digital mammograms in Kundel H (ed). *Medical Imaging 1997: Image Perception*, Proceedings of SPIE 3036. 1997; pp. 198-204.
8. Sittek H, Perlet C, Helmberger R et al. Computer-assisted analysis of mammograms in routine clinical diagnosis. *Radiologe* 1998; 38:848-52
9. Freer TW & Ulissey MJ. Screening Mammography with computer-aided detection: prospective study of 12,860 patients in a community breast centre. *Radiol.* 2001; 220(3):781-6
10. Thurfjell E, Thurfjell G, Egge E, Bjurstam N. Sensitivity and specificity of computer-assisted breast cancer detection in mammography screening. *Acta Radiol.* 1998; 39: 384-388
11. Cowley H and Gale A, PERFORMS and Mammographic Film Reading Performance: Radiographers, Breast Physicians and Radiologists. Report for the Workforce Issues in the Breast Screening Programme Meeting, Inst of Behavioural Sciences, Univ of Derby, 1999.
12. Pauli R, Hammond S and Ansell J. Comparison of radiographer/radiologist double film reading with single reading in breast cancer screening. *J Med Screen* 1996; 3:18-22

Breast Density Estimation: Correlation of Mammographic Density and MR Volumetric Density

Heang-Ping Chan, Lubomir M. Hadjiiski, Marilyn A. Roubidoux, Mark A. Helvie, Sophie Paquerault, Berkman Sahiner, Jun Wei, Chuan Zhou, Thomas Chenevert, Mitchell M. Goodsitt

Department of Radiology, University of Michigan, Ann Arbor, MI 48109
Chanhp@umich.edu

Abstract. Studies have demonstrated a strong correlation between mammographic breast density and breast cancer risk. Mammographic breast density may therefore be used as a surrogate marker for monitoring the response to treatment in studies of breast cancer prevention or intervention methods. In this study, we evaluated the accuracy of using mammograms for estimating breast density by analyzing the correlation between the percent mammographic dense area and the percent glandular tissue volume as estimated from MR images. A data set of 37 patients who had corresponding MR images and mammograms was collected. The glandular tissue regions in the MR slices were segmented by a semi-automatic method and the percent glandular tissue volume calculated. Mammographic breast density was estimated by an automated image analysis program. It was found that the correlation between the percent dense area of the CC and MLO views and the percent volumetric fibroglandular tissue on MR images was 0.93 and 0.91, respectively, with a mean bias of 4.4%. The high correlation indicates the usefulness of mammographic density as a surrogate for breast density estimation.

1. Introduction

Previous studies have shown that there is a strong positive correlation between breast parenchymal density on mammograms and breast cancer risk [1-3]. The relative risk is estimated to be about 4 to 6 times higher for women whose mammograms have parenchymal densities over 60% of the breast area, as compared to women with less than 5% of parenchymal densities. The change in mammographic breast density is therefore often used as an indicator for monitoring the effects of preventive or interventional treatment of breast cancer.

Breast cancer risk is expected to depend on the volume of glandular tissue in the breast. Mammographic density is a projection of the volume of glandular tissue onto the two-dimensional image plane. To better understand the correlation between mammographic density and breast cancer risk, it is important to investigate the relationship between the projected areal density on mammograms and the volume of glandular tissue in the breast. In this study, we investigate this relationship by analyzing the percent volumetric glandular tissue in magnetic resonance (MR) images and the percent dense area in corresponding mammograms for the same breasts.

2. Materials and Methods

Our data set consisted of corresponding MR breast images and mammograms from 37 patients acquired between detection and biopsy. The MR image series used in this study, which included coronal 3D T_1-weighted pre-contrast images (coronal sections 2-5 mm thick, 32 slices; 3D Spoiled Gradient-Recalled Echo (SPGR); TE=3.3ms; TR=10ms, Flip=40°, matrix=256x128, FOV=28-32cm right/left, 14-16cm superior/inferior, scan time=2 min 38 sec) was part of a dynamic breast MRI study. This 3D SPGR sequence produced full volume coverage of both breasts with contiguous image slices. An example of images from one breast is shown in Fig. 1. Although this is not the optimal pulse sequence for separating water and fat, the fibroglandular parenchyma (~water) and fatty tissue are well separated with this heavily T_1-weighted acquisition and therefore the series was chosen for this study.
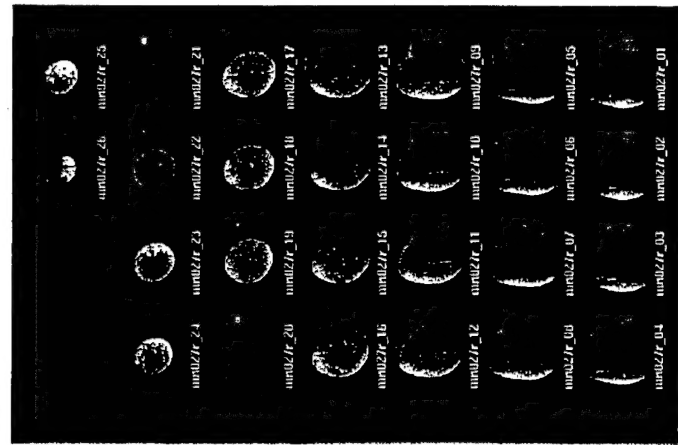

Fig. 1. MR images of the right breast of a patient. The two-view mammogram of the same breast is shown in Fig. 2.

We have developed a graphical user interface that displays the MR series and the corresponding mammogram of each breast. The interface allows the user to perform a combination of manual and automatic operations to segment the MR images. Each MR slice is first thresholded to separate the breast from the surrounding region. For slices close to the chest wall where no clear boundary can be seen, the boundary is manually drawn and evaluated by radiologists. Background correction [4] is employed to correct for the non-

uniformity across the breast area due to the breast coil. The histogram of the voxel values in the breast region is then formed and interactive thresholding is used to segment the fibroglandular tissue from the fatty tissue. A morphological erosion operation along the breast boundary then excludes the skin voxels from the calculation of the fibroglandular tissue area in each slice. Finally, an integration of the fibroglandular voxels in all slices relative to the breast volume provides the percent volumetric fibroglandular tissue in the breast.

We have previously developed an automated image analysis tool (Mammographic Density ESTimator) to assist radiologists in estimating mammographic breast density [5]. MDEST performs dynamic range compression, breast boundary tracking, pectoral muscle segmentation for the MLO view, automatic thresholding based on a gray level histogram analysis, and calculates the percent dense area on a mammogram. We found that the correlation between the computer-estimated percent dense area and radiologists' manual segmentation was 0.94 and 0.91, respectively, for CC and MLO views, with a mean bias of less than 2%. An example of a mammogram segmented by MDEST is shown in Fig. 2.
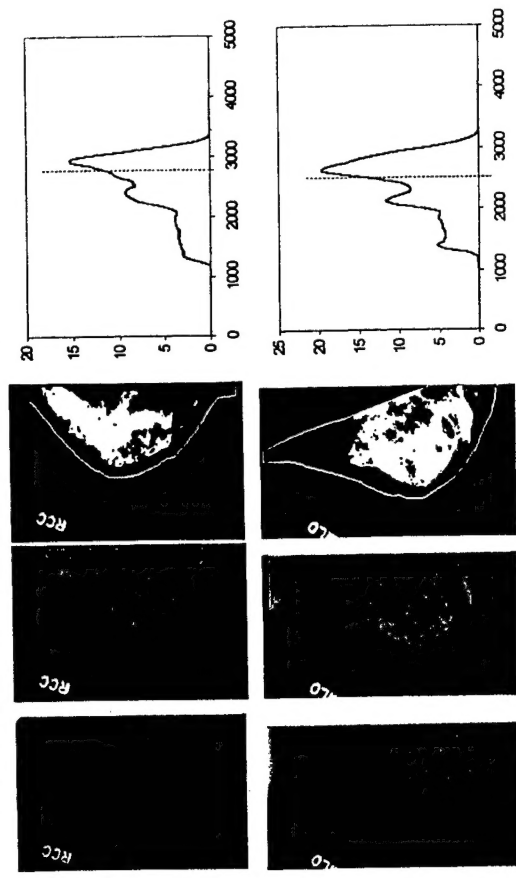

Fig. 2. Automated breast density segmentation from mammograms. Upper row: CC view. Lower row: MLO view.

3. Results

Scatter plots of the percent volumetric fibroglandular tissue versus the percent dense area on mammograms are shown in Fig. 3(a) and 3(b) for the CC- and MLO-view mammograms, respectively. The correlation of percent dense area of the CC and MLO views with the percent volumetric fibroglandular tissue on MR images was found to be 0.93 and 0.91, respectively, with a mean bias of 4.4%.
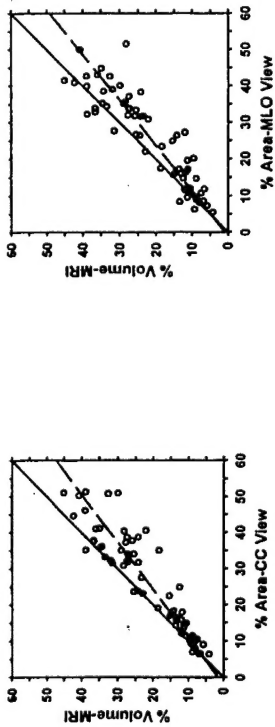
Statistical Characterization of Normal Curvilinear Structures in Mammograms

Carolyn Evans, Keith Yates and Michael Brady

Medical Vision Laboratory, Department of Engineering Science, University of Oxford, OX1 3PJ, UK. - {cje,jmb}@robots.ox.ac.uk
Department of Computing and Mathematics, Manchester Metropolitan University, Chester Street Manchester M1 5GD - K.Yates@mmu.ac.uk

Abstract. Curvilinear structures (CLS) in mammograms physically correspond to milk ducts, blood vessels, Cooper's ligaments and spicules in the breast. All of these structures, bar spicules, are features of normal breast tissue. Spicules are highly indicative of breast cancer when found near the boundary of a mammographic density.

In this paper we develop a statistical characterization of normal CLS, to be used to identify any normal CLS near the boundary of a mammographic density and avoid mis-diagnosis. Six shape features, were calculated from each CLS description to form a data set. Principal component analysis of the six-dimensional data set revealed that the majority of information was concentrated in the first two dimensions - the first two principal components. The distribution of normal CLS shape data in these first two dimensions was modeled using a Gaussian Mixture Model (GMM)

1 Introduction

The aim of our work is to obtain a model of the multivariate distribution of shape of CLS found in normal breast tissue so it can be used to diagnose how 'normal' a linear structure appears. We aim to model the shape distribution of normal CLS, rather than the spicules, because we can guarantee that a CLS which does not intersect a known abnormal region is (by definition) normal. We can make no such claim for CLS that intersect abnormal regions; they may be normal, but they may be spicules. We know the positions of all abnormal regions in the mammograms used in this study because they are provided as part of the University of South Florida's database [1].

2 Method

In order to characterize statistically normal CLS, we must perform the following series of tasks in order to gather the CLS shape information.

Fig. 3. Correlation of % volumetric fibroglandular tissue on MR images with % dense area on mammograms for 37 patients. The left and right breasts are plotted as separate data points on each graph. The dash lines are linear least squares fits to the data points.

4. Conclusion

Mammographic density is highly correlated with the volumetric fibroglandular tissue in the breast, indicating its usefulness as a surrogate for breast density estimation. The computerized image analysis tool, MDEST, is useful for estimation of mammographic density. The automated analysis is expected to contribute to the understanding of the relationship of mammographic density to breast cancer risk, detection, and prognosis, and to the prevention and treatment of breast cancer.

Acknowledgements

References

1. J. Brisson, R. Verreault, A. S. Morrison, D. Tennina and F. Meyer, "Diet, mammographic features of breast tissue, and breast cancer risk," Am. J. Epidemiology 130, 14-24 (1989).
2. A. F. Saftlas, R. N. Hoover, L. A. Brinton, M. Szklo, D. R. Olson, M. Salane and J. N. Wolfe, "Mammographic densities and risk of breast cancer," Cancer 67, 2833-2838 (1991).
3. N. F. Boyd, G. A. Lockwood, J. W. Byng, D. L. Tritchler and M. J. Yaffe, "Mammographic densities and breast cancer risk," Cancer Epidemiology Biomarkers & Prevention 7, 1133-1144 (1998).
4. B. Sahiner, H. P. Chan, N. Petrick, D. Wei, M. A. Helvie, D. D. Adler and M. M. Goodsitt, "Classification of mass and normal breast tissue: A convolution neural network classifier with spatial domain and texture images," IEEE Trans Med Imag 15, 598-610 (1996).
5. C. Zhou, H. P. Chan, N. Petrick, M. A. Helvie, M. M. Goodsitt, B. Sahiner and L. M. Hadjiiski, "Computerized image analysis: Estimation of breast density on mammograms," Med Phys 28, 1056-1069 (2001).